

THE ASTROPHYSICAL JOURNAL, 168: 283-311, 1971 September 1
 © 1971 The University of Chicago All rights reserved Printed in U S A

RADIATION FROM A HIGH-TEMPERATURE, LOW-DENSITY PLASMA: THE X-RAY SPECTRUM OF THE SOLAR CORONA

WALLACE H. TUCKER AND MARVIN KOREN*

American Science and Engineering, Cambridge, Massachusetts 02142

Received 1971 February 13

ABSTRACT

The results of calculations of the 0.5–70 Å X-ray spectrum of a high-temperature, low-density plasma are presented. The temperature range is 6×10^5 °– 10^8 ° K, and the elemental abundances characteristic of the solar corona have been assumed. We have considered the processes of line emission following electron collisional excitation, radiation resulting from recombination, bremsstrahlung, and two-photon decay following the excitation of the metastable 2S state in hydrogenic and helium-like ions.

I. INTRODUCTION

We present here the results of calculations of the 0.5–70 Å X-ray spectrum of high-temperature, low-density plasma having an electron temperature in the range 6×10^5 °– 10^8 ° K and elemental abundances equal to those generally believed to exist in the solar corona. We have made the usual assumptions of steady-state conditions and negligible absorption and have considered the processes of line emission following electron collisional excitation, radiation resulting from recombination, bremsstrahlung, and the two-photon decay following the excitation of the metastable 2S state in hydrogenic and helium-like ions.

Apart from differences in the values assumed for some of the cross-sections, these calculations differ from previous ones (Culhane 1969; Landini and Fossi 1970, and references cited therein) primarily in that we have included a large number of lines, some 459 in all, and in the consideration of the two-photon process. It turns out that this latter process is not too important, so our results for the continuous spectrum are not significantly different from those of Culhane (1969) and Landini and Fossi (1970). However, because of the much larger number of lines considered, our results for the total spectrum differ somewhat from those of Landini and Fossi (1970) with regard to both the relative importance of line radiation versus continuum radiation and the detailed shape of the spectrum.

In § II the basic assumptions and equations employed in the calculations are discussed, and in § III the results are presented in the form of tables and graphs.

II. BASIC EQUATIONS AND ASSUMPTIONS

a) *The Discrete Spectrum*

In a low-density plasma such as the solar corona, line emission results from downward radiative transitions following the population of an excited level either by recombination or by inelastic collisions. The emitted photon may be resonance absorbed and re-emitted, but we assume here that it eventually escapes from the hot plasma.

i) *Line Emission following Electron Collisional Excitation*

The X-ray emission lines in the coronal spectrum are produced primarily as a result of this process. The energy emitted per unit volume per unit time due to excitation of level n followed by a downward transition to a level n' is given by

$$dE_{L,Z,z}(nn')/dt dV = P_{L,Z,z}^{\text{ex}}(nn') = N_e N_{Z,z} E_{Z,z}(nn') \langle Q_{Z,z}(n)v \rangle, \quad (1)$$

* Present address: U.S. Army Strategic Communications Command, Fort Huachuca, Arizona

where N_e is the electron density, $N_{Z,z}$ is the density of ion species Z,z , $E_{Z,z}(nn')$ is the energy of the line, $Q_{Z,z}(n)$ is the cross-section for excitation of the level n from the ground state, v is the electron velocity, and the angular brackets denote an average over a Maxwellian distribution of electron velocities. Excitation cross-sections are often expressed in terms of the collision strength Ω :

$$Q_{Z,z}(n) = \pi a_0^2 \Omega_{Z,z}(n, k_i^2) / k_i^2, \quad (2)$$

where k_i^2 is the incident electron energy in rydbergs and a_0 is the Bohr radius. Since Ω is a slowly varying function of energy, the rate of radiative energy loss per unit volume for species Z,z and transition $n-n'$ is given approximately by

$$\begin{aligned} P_{L,Z,z}^{\text{ex}}(nn', T) &= 1.86 \times 10^{-19} T_6^{-1/2} N_e N_{Z,z} \langle \Omega(n) \rangle [E(nn') / I_H] B(nn') \\ &\times \exp [-E_{Z,z}(n)/kT] \text{ ergs cm}^{-3} \text{ sec}^{-1}, \end{aligned} \quad (3)$$

where T_6 is the electron temperature in millions of degrees, $\langle \Omega \rangle$ is an appropriate average value of the collision strength which is approximately equal to its value at $k_i^2 = 1.5 E(n)$; $E_{Z,z}(n)$ is the excitation energy of the level n ; I_H is the ionization potential of hydrogen; and $B(nn')$ is a branching ratio giving the fraction of decays of excited state n that lead to the final state n' .

In order to compute the intensity of line radiation as a function of temperature, one needs to know the density, the abundances of the elements, the ionization equilibrium, the collision strengths, the wavelengths of the lines, and the excitation energies.

Abundances of the elements appropriate to the solar corona were taken to be (Pottasch 1967; Jordan 1966a, b): $A(\log N) = \text{H}(12.00)$, $\text{He}(11.30)$, $\text{C}(8.70)$, $\text{N}(7.80)$, $\text{O}(8.50)$, $\text{Ne}(7.60)$, $\text{Mg}(7.50)$, $\text{Si}(7.70)$, $\text{S}(7.30)$, $\text{Ca}(6.30)$, $\text{Fe}(7.70)$, and $\text{Ni}(6.70)$.

As pointed out by Pottasch, the abundances relative to hydrogen are uncertain by about a factor of 3 due to uncertainties in the methods for determining the hydrogen number density. We have adopted a value for $N(\text{Si})/N(\text{H})$ of 5×10^{-4} , which is the value suggested by Jordan and used by Landini and Fossi (1970) and Culhane (1969).

Jordan's (1969, 1970) calculations of the ionization equilibrium were used. She included the processes of collisional ionization from the ground state, collisional excitation followed by autoionization, radiative recombination, and dielectronic recombination reduced by a density-dependent term. This latter term was computed for a particular model for the solar chromosphere and corona according to which $\log N_e T \approx 14.90$ for $\log T \lesssim 6.10$, $\log N_e = 8.30$ for $\log T \geq 6.10$.

A comparison of her results with results of similar calculations in which the full dielectronic-recombination rate was used indicates that the population of a given ionization state may sometimes be changed by as much as a factor of 4, but for ions which make important contributions to the X-ray spectrum of the solar corona the effect is usually less than 10–20 percent. It should also be noted that for these ions, the difference between the results of Jordan and other similar calculations (Allen and Dupree 1969; Cox and Tucker 1969) is also small, not more than 20 percent.

For calcium, we used the ionization-equilibrium calculations of Burgess and Faulkner (private communication). In these calculations the processes of collisional ionization from the ground state, radiative recombination, and dielectronic recombination were included.

In Table 1 the atomic data used to compute the line intensities are listed. The energy levels needed for the calculations were obtained from Kelly (1968), Chapman (1969), Connerade (1970), Moore (1949, 1952), Widing and Sandlin (1968), Walker and Rugge (1970), Rugge and Walker (1970), and Evans and Pounds (1968). Where necessary, energy levels were determined by isoelectronic interpolation and extrapolation. The specific reference for each line is given in Table 1. The lines referenced WS (Widing and Sandlin), RW (Rugge and Walker) and EP (Evans and Pounds) have been observed in the solar corona.

TABLE 1
ATOMIC DATA USED TO COMPUTE THE LINE INTENSITIES

Ion	Transition	Wavelength (Å)	Excitation Energy (eV)	Effective Collision Strength	Reference*
C VI.....	$1s-np$	26.4	470	0.003	(K)
	$1s-4p$	27.0	459	0.002	
	$1s-3p$	28.5	435	0.006	WS
	$1s-2p$	33.7	368	0.042	(K)
C V.....	$1s^2-1s np$	32.8	378	0.008	(K)
	$1s^2-1s4p$	33.4	371	0.006	(K)
	$1s^2-1s3p$	35.0-35.1	353	0.014	WR
	$1s^2-1s2p(^1P)$	40.3	308	0.084	WS
	$1s^2-1s2p(^3P)$	40.7	306	0.008	(M)
N VII.....	$1s^2-1s2p(^3S)$	41.5	300	0.089	(M)
	$1s-np$	19.4	639	0.002	
	$1s-4p$	19.8	626	0.002	
	$1s-3p$	20.9	593	0.005	RW
N VI.....	$1s-2p$	24.8	500	0.031	RW
	$1s^2-1s np$	23.3	532	0.005	(K)
	$1s^2-1s4p$	23.8	521	0.004	
	$1s^2-1s3p$	24.9-25.0	496	0.010	(K)
O VIII.....	$1s^2-1s2p(^1P)$	28.8	430	0.056	(M)
	$1s^2-1s2p(^3P)$	29.1	425	0.010	(M)
	$1s^2-1s2p(^3S)$	29.5	420	0.063	(M)
	$1s-np$	14.8	837	0.002	RW
O VII.....	$1s-4p$	15.2	816	0.002	RW
	$1s-3p$	16.0	775	0.005	RW, EP (CO)
	$1s-2p$	19.0	653	0.023	RW, EP (CO)
	$1s^2-1s np$	17.4	713	0.004	RW
Ne X.....	$1s^2-1s4p$	17.8	697	0.004	RW
	$1s^2-1s3p$	18.7	663	0.009	RW, EP (CO)
	$1s^2-1s2p(^1P)$	21.6	575	0.056	WR, EP (CO)
	$1s^2-1s2p(^3P)$	21.8	570	0.010	WR, EP (CO)
Ne IX.....	$1s^2-1s2p(^3S)$	22.1	560	0.063	WR, EP (CO)
	$1s-np$	9.5	1305	0.0010	RW
	$1s-4p$	9.7	1280	0.00084	RW
	$1s-3p$	10.2	1215	0.0024	RW
Ne VIII.....	$1s-2p$	12.2	1020	0.015	RW, EP (CO)
	$1s^2-1s np$	10.8	1148	0.003	(K)
	$1s^2-1s4p$	11.0	1130	0.002	(K)
	$1s^2-1s3p$	11.6	1070	0.005	RW, EP (CO)
Mg XII.....	$1s^2-1s2p(^1P)$	13.4	925	0.030	RW, EP (CO)
	$1s^2-1s2p(^3P)$	13.6	912	0.008	RW, EP (CO)
	$1s^2-1s2p(^3S)$	13.7	905	0.025	WR
	$2s-nl$	52-65.9	188	0.050	(K)
Mg XI.....	$2s-4l$	67.4-74.6	165	0.050	(K)
	$1s-np$	6.6	1879	0.00076	(K)
	$1s-4p$	6.7	1850	0.00058	
	$1s-3p$	7.11	1740	0.0017	WR
Mg X.....	$1s-2p$	8.42	1470	0.010	RW, EP (CO)
	$1s^2-1s np$	7.30	1698	0.002	(K)
	$1s^2-1s4p$	7.47	1660	0.0016	(K)
	$1s^2-1s3p$	7.85-7.86	1570	0.0035	WR
Mg X.....	$1s^2-1s2p(^1P)$	9.17	1350	0.022	RW, EP (CO)
	$1s^2-1s2p(^3P)$	9.23	1340	0.007	RW, EP (CO)
	$1s^2-1s2p(^3S)$	9.31	1330	0.017	RW, EP (CO)
	$2l-nl$	33.8-43.0	290	0.04	(K)
Mg X.....	$2l-4l$	44.0-47.3	260	0.04	(K)
	$2s-3p$	57.9	214	0.037	WS
	$2p-3d$	63.2-63.3	215	0.09	WS
	$2p-3s$	65.7-65.9	208	0.045	WS

* Lines observed in solar corona: WS = Widing and Sandlin; WR = Walker and Rugge; RW = Rugge and Walker; EP = Evans and Pounds. Lines observed in laboratory or computed theoretically: (K) = Kelly; (C) = Chapman; (CO) = Connerade; (M) = Moore; (H) = Hydrogenic. Lines not referenced were obtained by extrapolation or interpolation.

TABLE 1—Continued

Ion	Transition	Wavelength (Å)	Excitation Energy (eV)	Effective Collision Strength	Reference*
Mg IX.....	$2s2l-2s\ nl'$	38–47	262	0.090	(K)
	$2s2l-2s4l'$	48–52	237	0.090	(K)
	$2s^2-2s3p$	62.8	196	0.092	WS
	$2s2p-2s3d(^3D)$	67.2	214	0.12	WS
	$2s2p-2s3d(^1D)$	72.3	201	0.12	WS
Mg VIII.....	$2s2l2l'-2s2l\ nl''$	46.5–53.5	232	0.26	(K)
	$2s2l2l'-2s2l4l''$	52.4–64.3	193	0.26	(K)
	$2s^22p-2s2p3p$	64.2–71.7	182	0.09	(K)
	$2s^22p-2s2p3d$	72.6–77.4	193	0.27	(K)
	$2p-3d$	75.0	165	0.32	WS
Mg VII.....	$2s2p^2-2s2p2l\ nl''$	55–66.8	186	0.33	(K)
	$2s^22p^2-2s2p^24p$	63.4	196	0.04	(K)
	$2s^22p^2-2s^22p4d$	68.0–71.8	173	0.16	(K)
	$2s2p^3-2s2p^4d,4s$	67.5–72.9	201	0.09	(K)
	$2s^22p^2-2s2p^3p$	77.0–81.0	186	0.11	(K)
Si XIV.....	$1s-np$	4.83	2567	0.00056	(K)
	$1s-4p$	4.95	2500	0.00043	(K)
	$1s-3p$	5.22	2460	0.0012	WR
	$1s-2p$	6.18	2000	0.0077	WR
Si XIII.....	$1s^2-1s\ np$	5.29	2344	0.002	(K)
	$1s^2-1s4p$	5.40	2290	0.001	(K)
	$1s^2-1s3p$	5.68	2180	0.0025	WR
	$1s^2-1s2p(^1P)$	6.65	1860	0.016	WR, EP (CO)
	$1s^2-1s2p(^3P)$	6.69	1850	0.006	WR, EP (CO)
	$1s^2-1s2p(^3S)$	6.74	1840	0.011	WR, EP (CO)
Si XII.....	$2l-nl'$	23.7–29.8	415	0.026	
	$2l-4l'$	30.6–32.8	378	0.026	
	$2s-3p$	40.9	303	0.029	WS
	$2p-3d$	44.2	304	0.065	WS
	$2p-3s$	45.6	296	0.033	WS
Si XI.....	$2s2l-2s\ nl'$	26.0–32.7	379	0.061	
	$2s2l-2s4l'$	33.3–36.2	357	0.061	
	$2s^2-2s3p$	43.8	283	0.066	WS
	$2s2p-2s3d(^3D)$	46.3	309	0.079	WS
	$2s2p-2s3d(^1D)$	49.2	293	0.079	WS
Si X.....	$2s2p-2s3s$	52.3	288	0.076	WS
	$2s2p2l-2s2p\ nl'$	30.0–34.2	362	0.12	
	$2s2p2l-2s2p4l'$	33.5–41.0	336	0.12	
	$2s^22p-2s2p3p$	48.0	258	0.074	(K)
	$2s2p^2-2s2p3d$	49.7–56.8	269	0.18	(K)
Si IX.....	$2p-3d$	50.6	244	0.21	WS
	$2s2p^2-2s2p3s$	53.5–60.5	271	0.090	
	$2s^22p-2s23s$	54.0	230	0.059	
	$2s2p^2-2s2p2lnl'$	35–40	310	0.10	
	$2s^22p^2-2s2p^24p$	38	326	0.02	
Si VIII.....	$2s^22p^2-2s^22p4d$	44.2	280	0.10	(K)
	$2s2p^3-2s2p^24d,s$	41–43	331	0.06	
	$2s^22p^2-2s2p^23p$	51–54	236	0.08	(K)
	$2s2p^3-2s2p^23d$	52.7–55.7	265	0.22	(K)
	$2p^2-2p3d$	55.3	222	0.52	WS
Si VII.....	$2s2p^3-2s2p^23s$	61.2	244	0.11	(K)
	$2p^2-2p3s$	61.7	201	0.14	WS
	$2s^22p^3-2s^22p^22p\ nd$	47.6	260	0.03	
	$2s2p^4-2s2p^3nd$	47.7	296	0.02	
	$2s^22p^3-2s^22p^24d$	50.0–52.4	242	0.04	(K)
Si VI.....	$2s2p^4-2s2p^34d$	52.5	275	0.03	
	$2s^22p^3-2s^22p^24s$	53.8	230	0.02	(K)
	$2s2p^4-2s2p^34s$	54.5	266	0.01	
	$2s^22p^3-2s2p^33p$	58.9	210	0.09	(K)
	$2p^3-2p^23d(^4P, ^4D)$	61.0	203	0.36	WS

TABLE 1—Continued

Ion	Transition	Wavelength (Å)	Excitation Energy (eV)	Effective Collision Strength	Reference*
Si VIII	$2p^3-2p^2\ 3d$ ($^2S, ^2P, ^2D, ^2F$) $2s^2p^4-2s^2p^33d$ $2p^3-2p^2\ 3s(^4P)$ $2p^3-2p^2\ 3s(^2P, ^2D)$ $2s^2p^4-2s^2p^3\ 3s$	61.4–65.8 67.3 69.8 70.5–74.2 76.0	195 223 177 172 202	0.36 0.26 0.10 0.10 0.13	(K) (K) (K) (K) (K)
Si VII	$2s^2p^4\ 2l-2s^2p^3\ 2lnl'$ $2s^2p^4\ 2l-2s^2p^3\ 2l4l'$ $2s^2\ 2p^4-2s^2p^5\ 3p$ $2p^4-2p^3\ 3d$ $2s^2p^5-2s^2p^4\ 3d$ $2p^4-2p^3\ 3s(^3P)$	50.5–56.5 57.3–65.6 64 68.0–73.4 65–72.5 79.5	219 202 193 176 227 156	0.11 0.11 0.11 0.23 0.34 0.08	(K) (K) (K) (K) (K) (K)
S XVI	$1s-np$ $1s-4p$ $1s-3p$ $1s-2p$	3.70 3.78 3.99 4.73	3340 3270 3100 2620	0.00043 0.00033 0.00094 0.0059	(K) (K) (K) WR
S XV	$1s^2-1s\ np$ $1s^2-1s4p$ $1s^2-1s3p$ $1s^2-1s2p(^1P)$ $1s^2-1s2p(^3P)$ $1s^2-1s2p(^3S)$	4.01 4.10 4.30 5.04 5.07 5.10	3080 3010 2870 2460 2450 2430	0.001 0.001 0.0019 0.012 0.005 0.008	WR WR WR
S XIV	$2l-nl'$ $2l-4l'$ $2s-3p$ $2p-3d$ $2p-3s$	17.6–22 22.6–24.2 30.2 32.6 33.8	557 509 406 409 398	0.02 0.02 0.02 0.05 0.02	
S XIII	$2s2l-2s\ nl'$ $2s2l-2s4l'$ $2s^2-2s3p$ $2s2p-2s3d$ $2s2p-2s3s$	19–21 24–26 31 33–35 37	519 489 387 412 394	0.043 0.043 0.047 0.11 0.054	
S XII	$2s2p2l-2s2p\ nl'$ $2s2p2l-2s2p4l'$ $2s^2p-2s2p3p$ $2s2p^2-2s2p3d$ $2p-3d$ $2s2p^2-2s2p3s$ $2p-2s$	22–23.9 23.4–28.7 33.3 34.7–39.8 35.4 37.4–42.4 37.8	494 456 350 366 352 359 328	0.084 0.084 0.052 0.13 0.15 0.063 0.041	
S XI	$2s2p^2\ 2l-2s2p2l\ nl'$ $2s2p^2\ 2l-2s2p2l4l'$ $2s^2p^2-2s2p^2\ 3p$ $2s2p^3-2s2p^2\ 3d$ $2p^2-2p3d$ $2s2p^2\ 2l-2s2p^2\ 2l3s$ $2s2p^3\ 2l-2s2p2l\ nl'$	24.6–26.8 25.4–28.8 34.2–36.2 35.2–37.3 37.0 41.0 28.0–31.4	441 450 336 378 326 316 396	0.067 0.067 0.054 0.15 0.35 0.17 0.11	
S X	$2s2p^3\ 2l-2s2p2l4l'$ $2s^2p^3-2s2p^3\ 3p$ $2p^3-2p^23d(^4P, ^4D)$ $2p^3-2p^23d$ ($^2S, ^2P, ^2D, ^2F$) $2s^2p^4-2s2p^3\ 3d$ $2p^3-2p^23s(^4P)$ $2p^3-2p^23s(^2P, ^2D)$ $2s^2p^4-2s2p^3\ 3s$	34.0–37.2 40.2 42.5 42.9–45.8 47 47.7 48.2–50.6 52.0 32.8–36.8 37.2–42.6 41.2–47 41.5 46.4–49.3 54.2–56.3 57.0	360 308 292 280 326 259 252 296 300 276 312 295 259 224 284	0.11 0.058 0.24 0.24 0.17 0.06 0.06 0.08 0.09 0.09 0.27 0.09 0.18 0.06 0.11	(K) (K)

TABLE 1—Continued

Ion	Transition	Wavelength (Å)	Excitation Energy (eV)	Effective Collision Strength	Reference*
S VIII.....	$2s2p^5 2l-2s2p^4 2l nl'$	37.6–41.6	298	0.07	(K)
	$2s2p^5 2l-2s2p^4 2l4l'$	44.4–47.8	270	0.07	(K)
	$2s^22p^5-2s2p^5 3p$	46	270	0.07	
	$2p^5-2p^4 3d$	51.2–54.6	234	0.44	(K)
	$2s2p^6-2s2p^6 3d$	58.5	212	0.21	
	$2p^6-2p^5 3s$	59.2–64.3	201	0.62	(K)
	$2s2p^6-2s2p^6 3s$	65.0	191	0.09	(K)
S VII.....	$2s^22p^6-2s2p^5 2l nl'$	44–50	247	0.30	(K)
	$2s^22p^6-2s2p^5 2l4l'$	51.8–54.9	233	0.30	(K)
	$2s^22p^6-2s2p^6 3p$	55	225	0.40	
	$2p^6-2p^5 3d$	60.8	204	0.30	(K)
	$2p^6-2p^5 3s$	72.4	171	0.79	(K)
Ca xx.....	$1s-np$	2.3	5250	0.00028	
	$1s-4p$	2.4	5150	0.00021	
	$1s-3p$	2.54	4860	0.00060	
	$1s-2p$	3.02	4100	0.0037	
Ca xix.....	$1s^2-1s np$	2.5	4850	0.0007	
	$1s^2-1s4p$	2.6	4750	0.0006	
	$1s^2-1s3p$	2.70	4570	0.0012	
	$1s^2-1s2p(^1P)$	3.18	3900	0.008	
	$1s^2-1s2p(^3P)$	3.20	3880	0.004	
	$1s^2-1s2p(^3S)$	3.22	3850	0.005	
Ca xviii.....	$2l-nl'$	11–12	890	0.01	
	$2l-4l'$	14–15	811	0.01	
	$2s-3p$	18	650	0.01	
	$2p-3d$	19–20	654	0.03	
	$2p-3s$	21	635	0.01	
Ca xvii.....	$2s2l-2s nl'$	11–13	896	0.03	
	$2s2l-2s4l'$	14–16	845	0.03	
	$2s2l-2s3l'$	19–22	701	0.13	
Ca xvi.....	$2s2p2l-2s2p nl'$	12.3–13	884	0.04	
	$2s2p2l-2s2p4l'$	12.7–15	816	0.04	
	$2s2p2l-2s2p3l'$	17.2–19.5	608	0.23	
Ca xv.....	$2s2p^2 2l-2s2p2l nl'$	13.9–15.1	780	0.038	
	$2s2p^2 2l-2s2p2l4l'$	14.3–16.3	795	0.038	
	$2s^2 2p^2-2s2p^2 3p$	19.3–20.4	594	0.030	
	$2s2p^3-2s2p^2 3d$	19.9–21.1	667	0.085	
	$2p^2-2p3d$	20.9	560	0.20	
	$2s2p^2 2l-2s2p3s2l$	23.2	560	0.096	
Ca xiv.....	$2s2p^3 2l-2s2p2l nl'$	15.3–17.2	725	0.060	
	$2s2p^3 2l-2s2p2l4l'$	18.7–20.4	658	0.060	
	$2s^2 2p^3-2s2p^3 3p$	22.0	564	0.032	
	$2p^3-2p^2 3d$	23.2–25	524	0.26	
	$2s2p^4-2s2p^3 3d$	25.8	595	0.093	
	$2p^3-2p^2 3s$	26.2–27.8	467	0.066	
	$2s2p^4-2s2p^3 3s$	28.5	540	0.044	
Ca xiii.....	$2s2p^4-2s2p^3 2l nl'$	17.2–19.2	572	0.047	
	$2s2p^4 2l-2s2p^3 2l4l'$	19.4–22.2	525	0.047	
	$2s^22p^4-2s2p^6 3p$	21.6	503	0.047	
	$2p^4-2p^3 3d$	24.2–25.8	494	0.094	
	$2s2p^5-2s2p^4 3d$	21.9–24.5	595	0.14	
	$2p^4-2p^3 3s$	28.3–29.4	426	0.031	
	$2s2p^5-2s2p^4 3s$	29.8	540	0.057	
Ca xii.....	$2s2p^5 2l-2s2p^4 2l nl'$	18.8–20.8	596	0.035	
	$2s2p^5 2l-2s2p^4 2l4l'$	22.2–23.9	540	0.035	
	$2s^22p^5-2s2p^6 3p$	23	540	0.035	
	$2p^5-2p^4 3d$	26.7–27.3	459	0.22	
	$2s2p^6-2s2p^5 3d$	29.2	424	0.11	
	$2p^5-2p^4 3s$	31.6–32.7	384	0.31	
	$2s2p^6-2s2p^5 3s$	32.5	382	0.045	

TABLE 1—Continued

Ion	Transition	Wavelength (Å)	Excitation Energy (eV)	Effective Collision Strength	Reference*
Ca xi.....	$2s^2 2p^6 - 2s 2p^5 2l nl'$	21–24	520	0.14	
	$2s^2 2p^6 - 2s 2p^5 2l 4l'$	23.6–26.7	477	0.14	
	$2s^2 2p^6 - 2s 2p^5 3p$	27.0	459	0.19	
	$2p^6 - 2p^5 3d$	30.4–31.2	401	0.14	
	$2p^6 - 2p^5 3s$	35.2	350	0.38	
Fe xxvi.....	$1s - np$	1.40	8840	0.00016	(H)
	$1s - 4p$	1.43	8650	0.00012	
	$1s - 3p$	1.51	8190	0.00036	(H)
	$1s - 2p$	1.79	6900	0.0022	(H)
Fe xxv.....	$1s^2 - 1s np$	1.50	8400	0.0004	(C)
	$1s^2 - 1s 4p$	1.51	8200	0.0003	
	$1s^2 - 1s 3p$	1.59	7760	0.0008	(C)
	$1s^2 - 1s 2p(^1P)$	1.87	6630	0.0045	
	$1s^2 - 1s 2p(^3P)$	1.88	6600	0.0026	
	$1s^2 - 1s 2p(^3S)$	1.89	6561	0.0022	
Fe xxiv.....	$2l - nl'$	6.06–7.21	1720	0.0071	
	$2l - 4l'$	8.35	1480	0.0071	(C)
	$2s - 3p$	10.8	1150	0.0095	CO
	$2p - 3d$	11.2	1150	0.018	(C)
	$2p - 3s$	11.4	1130	0.0086	(C)
Fe xxiii.....	$2s 2l - 2s nl'$	6.3–8.00	1550	0.0076	
	$2s 2l - 2s 4l'$	8.45–8.86	1430	0.0076	(C)
	$2s^2 - 2s 3p$	11.2	1110	0.010	(C)
	$2s 2p - 2s 3d(^3D)$	11.5	1150	0.0095	(C)
	$2s 2p - 2s 3d(^1D)$	11.8	1130	0.0095	(C)
	$2s 2p - 2s 3s$	12.0	1110	0.0095	(C)
Fe xxii.....	$2s 2p 2l - 2s 2p nl'$	6.91–7.89	1560	0.03	
	$2s 2p 2l - 2s 2l 4l'$	7.72–9.45	1440	0.03	
	$2s^2 2p - 2s 2p 3p$	11.5	1110	0.024	CO
	$2s 2p^2 - 2s 2p 3d$	11.5–13.1	1150	0.042	
	$2p - 3d$	11.9	1040	0.047	(C)
	$2s 2p^2 - 2s 2p 3s$	12.3–13.9	1130	0.026	
	$2s^2 2p - 2s^2 3s$	12.4	1000	0.012	(C)
Fe xxI.....	$2s^2 2p^2 - 2s 2p^2 np$	7.4	1470	0.007	
	$2s^2 2p^2 - 2s 2p^2 4p$	7.9	1550	0.0072	
	$2s 2p^3 - 2s 2p^2 nd, s$	8.0	1470	0.012	
	$2s^2 2p^2 - 2s^2 2p nd$	8.3	1470	0.019	
	$2s 2p^3 - 2s 2p^2 4d, s$	8.55–8.95	1330	0.012	
	$2s^2 2p^2 - 2s^2 2p 4d$	9.81	1570	0.019	CO
	$2s^2 2p^2 - 2s 2p^2 3p$	11.6–12.0	1120	0.026	CO
	$2s 2p^3 - 2s 2p^2 3d$	11.7–12.3	1260	0.046	CO
	$2p^2 - 2p 3d$	12.4–12.7	1050	0.11	CO
	$2s 2p^3 - 2s 2p^2 3s$	12.9	1160	0.028	
Fe xx.....	$2p^2 - 2p 3s$	13.0–13.5	955	0.026	CO
	$2p^3 - 2p^2 nd(4)$	9.2	1330	0.008	
	$2p^3 - 2p^2 nd(2)$	9.6	1330	0.008	
	$2p^3 - 2p^2 4d(4)$	9.7	1270	0.008	
	$2p^3 - 2p^2 4d(2)$	10.2–10.5	1270	0.008	CO
	$2s 2p^4 - 2s 2p^3 nd$	10.2	1330	0.007	
	$2s 2p^4 - 2s 2p^3 4d$	10.7	1270	0.007	
	$2s^2 2p^3 - 2s 2p^3 3p$	12.0–12.7	1100	0.027	CO
	$2p^3 - 2p 3d(^4P, ^4D)$	13.4	1040	0.056	CO
	$2p^3 - 2p^2 3d(^2S, ^2P, ^2D, ^2F)$	13.4–14.4	1000	0.056	CO
Fe xix.....	$2s 2p^4 - 2s 2p^3 3d$	14.7	1160	0.050	
	$2p^3 - 2p^2 3s(^4P)$	15.2	925	0.014	
	$2p^3 - 2p 3s(^2P, ^2D)$	15.4–16.3	910	0.014	
	$2s 2p^4 - 2s 2p^3 3s$	16.6	1060	0.025	
	$2s^2 2p^4 - 2s 2p^4 np$	8.6	1440	0.006	
	$2p^4 - 2p^3 nd$	9.5	1310	0.006	
	$2s 2p^5 - 2s 2p^4 nd$	9.7	1310	0.012	
	$2s^2 2p^4 - 2s 2p^4 4p$	9.7	1240	0.006	

TABLE 1—Continued

Ion	Transition	Wavelength (Å)	Excitation Energy (eV)	Effective Collision Strength	Reference*
Fe xix.....	$2s^2 p^6 - 2s^2 p^4 ns$	10.0	1240	0.006	CO
	$2p^4 - 2p^3 4d$	10.8	1240	0.006	
	$2s^2 p^6 - 2s^2 p^4 4d$	10.4	1240	0.012	
	$2s^2 p^6 - 2s^2 p^5 3p$	10.8	1020	0.029	
	$2s^2 p^6 - 2s^2 p^4 4s$	11.1	1240	0.006	
	$2p^4 - 2p^3 3d$	13.5–14.2	1000	0.030	
	$2s^2 p^6 - 2s^2 p^4 3d$	12.6–14.0	1210	0.055	
	$2p^4 - 2p^3 3s$	14.5–15.0	870	0.0083	
	$2s^2 p^6 - 2s^2 p^4 3s$	15.2	1100	0.027	
	$2s^2 p^6 - 2s^2 p^6 np$	9.15	1340	0.007	
Fe xviii.....	$2p^6 - 2p^4 nd$	10.2	1210	0.012	CO
	$2p^6 - 2p^4 ns$	10.4	1210	0.016	
	$2s^2 p^6 - 2s^2 p^6 ns$	10.7	1340	0.007	
	$2s^2 p^6 - 2s^2 p^6 nd$	10.9	1340	0.008	
	$2s^2 p^6 - 2s^2 p^5 4p$	10.9	1140	0.007	
	$2p^6 - 2p^4 4d$	12.2	1020	0.012	
	$2p^6 - 2p^4 4s$	12.4	1020	0.016	
	$2s^2 p^6 - 2s^2 p^5 3p$	13.4	1110	0.025	
	$2s^2 p^6 - 2s^2 p^4 4d$	13.0	1140	0.008	
	$2s^2 p^6 - 2s^2 p^4 4s$	13.7	1140	0.007	
Fe xvii.....	$2p^6 - 2p^4 3d$	14.3–14.4	862	0.088	RW, EP (CO)
	$2s^2 p^6 - 2s^2 p^5 3d$	15.4	872	0.058	
	$2p^6 - 2p^4 3s$	15.6–16.0	796	0.128	
	$2s^2 p^6 - 2s^2 p^6 3s$	16.2	785	0.050	
	$2s^2 p^6 - 2s^2 p^6 np$	9.9	1250	0.02	
	$2p^6 - 2p^5 nd$	10.1	1230	0.01	
	$2s^2 p^6 - 2s^2 p^6 4p$	11.0	1130	0.02	
	$2p^6 - 2p^5 ns$	11.1	1120	0.02	
	$2s^2 p^6 - 2s^2 2p^5 4d$	12.3	1010	0.03	
	$2p^6 - 2p^5 4s$	12.7	930	0.02	
Fe xvi.....	$2s^2 2p^6 - 2s^2 p^6 3p$	13.8	895	0.130	RW, EP (CO)
	$2s^2 2p^6 - 2s^2 2p^5 3s(^1P)$	15.0	824	0.06	
	$2s^2 2p^6 - 2s^2 2p^5 3d(^3D)$	15.3	806	0.047	
	$2s^2 2p^6 - 2s^2 2p^5 3s(^3P)$	15.5	796	0.07	
	$2s^2 2p^6 - 2s^2 2p^5 3s(^1P)$	16.8	735	0.062	
	$2s^2 2p^6 - 2s^2 2p^5 3s(^3P)$	17.1	722	0.07	
	$2s^2 2p^6 - 3s - 2s^2 p^6 3s3p$	15.4	895	0.120	
	$2s^2 2p^6 - 3s - 2p^5 3s3d$	17.1	806	0.050	
	$2p^6 - 3s - 2s^2 2p^5 3s^2$	17.5	730	0.130	
	$3s - 5p$	37.1	334	0.007	
Fe xv.....	$3p - 5d$	40.0	344	0.02	(M)
	$3p - 5s$	42.5	326	0.009	
	$3d - 5f$	47.4	350	0.02	
	$3s - 4p$	50.3–54.2	244	0.04	
	$3p - 4d$	54.7	264	0.09	
	$3p - 4s$	63.7	232	0.05	
	$3d - 4f$	66.4	271	0.13	
	$2s^2 2p^6 - 3s^2 - 2s^2 p^6 3s^2 4l$	13–18	820	0.13	
	$2p^6 - 3s^2 - 2p^5 3s^2 4l$	14–17	807	0.23	
	$3s3l - 3s nl'$	27.2–41	332	0.28	
Fe xiv.....	$3s^2 - 3s4p$	52.9	234	0.26	WS
	$3s3p - 3s4d$	53.9	252	0.10	
	$3s3d - 3s4f$	70.0	177	0.08	
	$3s3p - 3s4s$	74.5	196	0.18	
	$3s3l3l' - 3s3l nl''$	31.7–56	221	0.20	
	$3s^2 3p - 3s3p4p$	56.2	220	0.086	
Fe xiii.....	$3s3p^2 - 3s3p4d$	58	282	0.20	WS
	$3s^2 3p - 3s^2 4d$	60.0	206	0.29	
	$3s3p^2 - 3s3p4s$	70	245	0.12	
	$3s^2 3p - 3s^2 4s$	71	175	0.078	
					WS

TABLE 1—Continued

Ion	Transition	Wavelength (Å)	Excitation Energy (eV)	Effective Collision Strength	Reference*
Fe XIII.....	$3s^3p^3l3l'-3s3p3l\ nl''$	34.2-59	210	0.15	
	$3s^3p^3-3s3p^2\ 4d$	60	271	0.24	
	$3s^23p^2-3s^23p4d$	65	191	0.61	
	$3s3p^3-3s3p^2\ 4s$	70	241	0.13	
	$3s^23p^2-3s^23p4s$	76.0	163	0.17	WS (H) (H)
Ni XXVIII.....	$1s-np$	1.21	10300	0.00016	
	$1s-4p$	1.24	10000	0.00012	
	$1s-3p$	1.31	9450	0.00031	
	$1s-2p$	1.55	8000	0.0019	
Ni XXVII.....	$1s^2-1s\ np$	1.29	9600	0.0004	
	$1s^2-1s4p$	1.30	9550	0.0003	
	$1s^2-1s3p$	1.37	9050	0.0007	
	$1s^2-1s2p(^1P)$	1.60	7750	0.0038	
	$1s^2-1s2p(^3P)$	1.61	7700	0.0023	
	$1s^2-1s2p(^3S)$	1.62	7650	0.0018	
Ni XXVI.....	$2l-nl'$	5.15-6.14	2010	0.0061	
	$2l-4l'$	7.10	1730	0.0061	
	$2s-3p$	9.20	1350	0.0081	
	$2p-3d$	9.52	1350	0.010	
	$2p-3s$	9.70	1320	0.0073	
Ni XXV.....	$2s2l-2s\ nl''$	5.40-6.76	1810	0.0064	
	$2s2l-2s4l'$	7.15-7.50	1670	0.0064	
	$2s^2-2s3p$	9.50	1300	0.0085	
	$2s2p-2s3d(^3D)$	9.75	1350	0.0081	
	$2s2p-2s3d(^1D)$	10.0	1320	0.0081	
	$2s2p-2s3s$	10.2	1300	0.0081	
Ni XXIV.....	$2s2p2l-2s2p\ nl'$	5.81-6.62	1860	0.025	
	$2s2p2l-2s2l4l'$	6.50-7.94	1710	0.025	
	$2s^22p-2s2p3p$	9.32	1320	0.020	
	$2s2p^2-2s2p3d$	9.65-11.0	1370	0.035	
	$2p-3d$	10.0	1240	0.040	
	$2s2p^2-2s2p3s$	10.4-11.7	1340	0.022	
	$2s^22p-2s^23s$	10.4	1190	0.010	
Ni XXIII.....	$2s2p^2\ 2l-2s2p2l\ nl'$	6.15-6.94	1760	0.031	
	$2s2p^2\ 2l-2s2p^24l$	6.60-7.70	1780	0.032	
	$2s^22p^2-2s2p^23p$	8.85-9.35	1340	0.022	
	$2s2p^3-2s2p^23d$	9.20-9.70	1510	0.038	
	$2p^2-2p3d$	9.60	1260	0.092	
	$2s2p^3-2s2p^23s$	10.6	1390	0.023	
	$2p^2-2p3s$	10.7	1150	0.022	
Ni XXII.....	$2s2p^3\ 2l-2s2p^2\ 2l\ nl'$	6.45-7.26	1710	0.027	
	$2s^22p^3\ 2l-2s2p^22l4l'$	7.90-8.60	1550	0.027	
	$2s^22p^3-2s2p^33p$	9.25	1330	0.022	
	$2p^3-2p^33d(^4P, ^4D)$	9.65	1260	0.046	
	$2p^3-2p^33d(^2S, ^2P, ^2D, ^2F)$	9.65-10.04	1210	0.046	
	$2s2p^4-2s2p^33d$	10.7	1400	0.041	
	$2p^3-2p^33s$	11.0-11.7	1120	0.024	
Ni XXI.....	$2s2p^4-2s2p^33s$	12.0	1280	0.021	
	$2s2p^42l-2s2p^32l\ nl'$	6.72-7.60	1460	0.023	
	$2s2p^4\ 2l-2s2p^32l4l'$	7.70-8.83	1350	0.023	
	$2s^22p^4-2s2p^63p$	8.60	1290	0.023	
	$2s2p^6-2s2p^43d$	8.75-9.70	1460	0.044	
	$2p^4-2p^33d$	9.15-9.86	1260	0.024	
	$2p^4-2p^33s$	10.6-11.6	1100	0.0066	
Ni XX.....	$2s2p^6-2s2p^43s$	11.8	1390	0.021	
	$2s2p^5\ 2l-2s2p^42l\ nl'$	7.40-8.25	1510	0.040	
	$2s2p^5\ 2l-2s2p^42l4l'$	10.1-10.8	1380	0.040	
	$2s^22p^6-2s2p^63p$	10.4	1380	0.020	
	$2p^6-2p^43d$	11.6	1070	0.071	
	$2s2p^6-2s2p^53d$	12.5-12.6	1080	0.047	
	$2p^6-2p^43s$	12.6-12.9	987	0.10	
	$2s2p^6-2s2p^53s$	13.1	973	0.040	

TABLE 1—Continued

Ion	Transition	Wavelength (Å)	Excitation Energy (eV)	Effective Collision Strength	Reference*
Ni xix.....	$2s^2 2p^6 - 2s2p^6 np$	8.1	1530	0.02	
	$2p^6 - 2p^6 nd$	8.3	1490	0.008	
	$2s^2 2p^6 - 2s2p^6 4p$	9.0	1370	0.02	
	$2p^6 - 2p^6 ns$	9.1	1360	0.02	
	$2p^6 - 2p^6 4d$	10.0	1240	0.008	
	$2s^2 2p^6 - 2s^2 2p^6 4d$	10.0	1240	0.024	RW, EP (CO)
	$2s^2 2p^6 - 2s^2 2p^6 3p$	10.3	1090	0.09	
	$2p^6 - 2p^6 4s$	11.0	1130	0.02	
	$2s^2 2p^6 - 2s^2 2p^6 3d(^1P)$	12.4	1010	0.00094	
	$2s^2 2p^6 - 2s^2 2p^6 3d(^3D)$	12.6	983	0.039	
	$2s^2 2p^6 - 2s^2 2p^6 3d(^3P)$	12.8	971	0.0010	
	$2s^2 2p^6 - 2s^2 2p^6 3s(^1P)$	13.8	897	0.05	
	$2s^2 2p^6 - 2s^2 2p^6 3s(^3P)$	14.3	881	0.06	
	$2s^2 2p^6 - 3s - 2s2p^6 3s nl$	10.5–14.5	1030	0.10	
Ni xviii.....	$2p^6 3s - 2p^5 3s nl$	11.3–13.7	1010	0.19	
	$3l - nl'$	20–37	335	0.11	
	$3s - 4p$	40.6–43.7	305	0.03	
	$3p - 4d$	44.2	330	0.07	
	$3p - 4s$	51.7	290	0.04	
	$3d - 4f$	53.5	339	0.11	
	$2s^2 2p^6 - 3s^2 - 2s2p^6 3s^2 4l$	10.4–14.4	943	0.10	
Ni xvii.....	$2p^6 3s^2 - 2p^5 3s^2 4l$	11.2–13.6	928	0.18	
	$3s3l - 3s nl'$	23.7–32.8	382	0.22	
	$3s^2 - 3s4p$	42.2	269	0.21	
	$3s3p - 3s4d$	45.6	290	0.08	
	$3s3d - 3s4f$	56.0	204	0.064	
	$3s3p - 3s4s$	59.5	225	0.14	
Ni xvi.....	$3s3l3l' - 3s3l nl''$	24.9–43	281	0.16	
	$3s^2 3p - 3s3p4p$	44	279	0.068	
	$3s3p^2 - 3s3p4d$	45.5	358	0.16	
	$3s^2 3p - 3s^2 4d$	47.0	262	0.23	
	$3s3p^2 - 3s3p4s$	55	311	0.094	
	$3s^2 3p - 3s^2 4s$	55.7	222	0.061	
Ni xv.....	$3s3p3l3l' - 3s3p3l nl''$	26.6–45	271	0.12	
	$3s3p^3 - 3s3p^2 4d$	46.6	350	0.19	
	$3s^2 3p - 3s^2 3p4d$	50	246	0.47	
	$3s3p^3 - 3s3p^2 4s$	54	311	0.10	
	$3s^2 3p - 3s^2 3p4s$	59.0	210	0.13	

For the sake of convenience, we often lumped several levels together. Thus, for example, the effective excitation energy for transitions to levels with principal quantum number n greater than or equal to 5 was assumed to be the energy of the $n = 5$ level, and the effective wavelength of the lines resulting from transitions from these levels to a lower-lying level was assumed to be equal to the wavelength of the transition from the $n = 5$ level. A similar procedure was also used for many of the transitions in complex ions with levels of the same n often being lumped together. We indicate in Table 1 the wavelength region over which these lines will be distributed.

Also given in Table 1 are “effective collision strengths” or the product of the collision strength Ω and the branching ratio B . The cross-sections for excitation of the $2p$ level of hydrogenic ions have been computed recently by Beigman, Vainshtein, and Vinogradov (1970). Their results for the excitation of the $2p$ level are in agreement with the results of Burgess (1961) to within about 20 percent. Values of the collision strength which approximate the results of Beigman *et al.* (1970) to within 30 percent were adopted,

i.e., $\langle \Omega(1s, 2p) \rangle = 1.5/Z^2$. The cross-sections for the excitation of the higher- n levels should scale approximately according to $f(n)/E(n)$, where $f(n)$ is the oscillator strength for the transition to level n from the ground state. Recent calculations by Krinberg (1970) for the hydrogen atom indicates that this is a good approximation. Hence, we have assumed that $\langle \Omega(1s, 3p) \rangle = 0.24/Z^2$, and $\langle \Omega(1s, 4p) \rangle = 0.084/Z^2$. All transitions to levels higher than $n = 5$ were lumped together and assigned the energy of the $n = 5$ level, and the collision strengths summed over all bound levels with $n \geq 5.5$ so that $\langle \Omega(1s, n \geq 5.5) \rangle = 0.11/Z^2$. For the allowed transitions in heliumlike ions, we scaled the collision strengths from the hydrogenic values according to $f(n)/E(n)$. Recently, it has become clear that magnetic-dipole ($^3S-^1S$) and intercombination ($^3P-^1S$) transitions are also important in heliumlike ions. Gabriel and Jordan (1969) have computed the expected intensity of these lines relative to the allowed ($^1P-^1S$) transitions, and we have used their values. The relative strength of the magnetic-dipole and the intercombination lines is a function of density except in the limit of very low densities $N_e \ll 10^9$. We have used this low-density limit in our calculations.

For lithiumlike ions, we used the results of Bely (1966a, b) for $2s-3l$ and $2s-4l$ excitations. For the excitation of levels with $n \geq 5$, the collision strengths were obtained in the same manner as for the highly excited states of hydrogen and heliumlike ions. For berylliumlike ions we assumed that the collision strength was equal to twice that of the corresponding lithiumlike ion. For boronlike ions we used the collision strengths calculated by Bely and Petrini (1970) for the excitation of $2p-nl$ transitions in lithiumlike ions. For the other ions containing from two to five $2p$ electrons in the ground state, we scaled the collision strengths from the boronlike values according to $f(n)/E(n)$. We used the results of Bely and Bely (1967) for the neonlike ions of iron and nickel, and those of Bely (1967) for the sodiumlike and magnesiumlike ions.

We have not considered the line emission resulting from the excitation of K -shell electrons of ions having one or more electrons in the $n = 2$ shell. For a Maxwellian gas such as we are considering here, the ratio of the power in these lines, $p(K)$, to the power in lines produced by excitation of heliumlike ions of the same species, $p(\text{He-like})$ is given approximately by

$$p(K)/p(\text{He-like}) \sim (N_z/N_{\text{He-like}})K(Z), \quad (4)$$

where $K(Z)$ is the K -fluorescence yield. It is a rapidly increasing function of Z ; e.g., $K(10) = 0.00963$; $K(16) = 0.06$; $K(26) = 0.30$. From equations (3) and (4) one sees that K -lines may be important in a narrow temperature range where $N(z) > N(\text{He-like})$ and $kT \sim E(K)$, the excitation energy for the inner-shell electron. Such a region does not exist except for the high- Z elements such as iron. In case of iron we find that the K -lines are important in the range $10^7 \leq T \leq 3 \times 10^7$ where they are at most about 20 percent as powerful as the heliumlike ions; outside this range they make a negligible contribution.

ii) Line Emission following Recombination

Line emission is also produced by the recombination of an electron excited state followed by a radiative transition to the ground state. For the steady-state conditions here, the number of recombinations must equal the number of ionizations, which will always be less than the number of excitations to the first excited state. Therefore, recombination radiation will not dominate the strong lines, and will usually be negligible. It can be shown that the line radiation resulting from radiative recombination is never important; however, in some cases line radiation following dielectronic recombination makes a nonnegligible contribution.

In the dielectronic recombination of an electron to an ion, the ion is stabilized by radiative transitions which eventually take the ion into the ground state. In general, this will involve the emission of at least two line photons, since the recombination pro-

cess leaves the ion in a doubly excited state n, n'' . The rate of radiative energy loss per unit volume due to the de-excitation of the ionic core in the state n can be approximated by the expression

$$P_{L,z,s}^{\text{di}}(nn'', n'n'', T) = N_e N_{z,s+1} E_{z,s}(nn') \alpha_{z,s}^{\text{di}}(n), \quad (5)$$

where $\alpha_{z,s}^{\text{di}}(n)$ is the rate coefficient for a dielectronic recombination in which the ionic core is excited to the state n . Note that, to the extent that the influence of the electron in state n'' can be neglected, the photons produced by this process will have an energy equal to the energy of photons resulting from the collisional excitation of the ion z to the state n . Using the general formula given by Burgess (1965) for $\alpha_{z,s}^{\text{di}}(n)$, one can relate $P_{L,z,s}^{\text{di}}(nn'', n'n'', T)$ to $P_{L,z,s}^{\text{ex}}(nn', T)$. The recent work of Shore (1969) indicates that for transitions in which the principal quantum number changes, Burgess's results are systematically too large. From the values tabulated by Shore for recombination to hydrogenic ions, one finds that Shore's recombination rates are related to Burgess's (α_B) by $\alpha \approx 3\alpha_B z^{-1.5}$ for $z > 6$. If we assume that this correction factor applies to all transitions in which the principal quantum number changes, then one has approximately

$$P_L^{\text{di}}/P_L^{\text{ex}} = R \approx 3 \times 10^4 T_6^{-1} (z + 1)^3 / [1 + 0.1(z + 1) + 0.01(z + 1)^2],$$

H-, He-like,

$$\approx 4 \times 10^{-5} T_6^{-1} (z + 1)^3, \quad \text{all others.} \quad (6)$$

From Jordan's (1969) ionization tables, one sees that, for hydrogenic and heliumlike ions, an ion z is not present in any appreciable concentration unless $T_6 \geq (z + 1)^2/100$, so that $R \leq 10^{-2} (z + 1)$ for $z \leq 15$, $R \leq 0.3/(z + 1)$ for $z \geq 15$. In an analogous manner we find for the other ions that $R \leq 10^{-2} (z + 1)$ for all $z \leq 25$.

The de-excitation of the electron in the highly excited state n'' is more complicated, since in this case one has to take into account the rate of population of the various l'' -levels of the state n'' , and the cascade probabilities to the lower states $n'''l'''$. In order to obtain a rough estimate of the relative importance of this process, we assume that the branching ratio for the rate of population of a state $n''l'''$ due to dielectronic recombination followed by cascade is equal to the branching-ratio rate for collisional excitation from the ground state. Then the ratio of the power produced in a given line by these processes can be approximated by

$$R^1(z) \approx R(z) \exp [(E_{z,s}(n'') - E_{z,s+1}(n')/kT)].$$

Since in general $E_{z,s}(n'') < E_{z,s+1}(n')$, we have $R^1(z) < R(z)$.

b) The Continuous Spectrum

The continuous X-ray spectrum of a hot, dilute, optically thin plasma is due to three processes: bremsstrahlung, radiative recombination, and two-photon decay of metastable states of hydrogen and helium.

i) Bremsstrahlung

In a hydrogenic approximation the energy emitted per unit time, volume, and wavelength interval due to encounters of Maxwellian electrons at a temperature T with ions of atomic number Z and charge z is given by

$$\frac{dE_{B,z,s}}{dt dV d\lambda} = \frac{dP_{B,z,s}}{d\lambda}(T) = \frac{2.04 \times 10^{-22}}{\lambda^2 T_6^{1/2}} z^2 N_e N_H \left(\frac{N_{Z,s}}{N_Z} \right) \left(\frac{N_Z}{N_H} \right) \approx \frac{1}{2 \pi v} \frac{\lambda^2 e^{-h/\lambda}}{\lambda^2 - 30} \times g_B(\lambda, z, T) \exp(-144/\lambda T_6) \text{ ergs (cm}^3 \text{ sec } \text{\AA})^{-1},$$

$$(h\nu_v = 2.41 \times 10^{17} \text{ Hz} = \frac{3 \times 10^{10}}{2.41 \times 10^{17}} \text{ cm} = 12.4 \text{ \AA})$$

$$\therefore 1 \text{ \AA} = \frac{1}{12.4} = .08 \text{ \mu m} \text{ or } .08 \frac{\text{m}}{\text{\AA}} \Rightarrow \frac{dE}{d\lambda} \approx \frac{2 \times 10^{-22}}{.08} n^2$$

where λ is in angstroms, and $g_B(\lambda, z, T)$ is an averaged bremsstrahlung Gaunt factor or order unity which has been computed by Karzas and Latter (1961). The bremsstrahlung spectrum of a plasma which is a mixture of a number of different ions is obtained by summing equation (7) over all Z, z . In the case of the solar corona it is possible to simplify this summation considerably since the principal contributors to the sum are hydrogen and helium, both of which are fully ionized in the solar corona. The contribution of the other elements to the sum is small, amounting to about 6 percent, and can, to a good approximation, be treated as a constant, independent of wavelength and temperature. One can then compute the bremsstrahlung spectrum from equation (7), using the values of the hydrogen and helium Gaunt factors obtained from the graphs given by Karzas and Latter (1961).

ii) Radiative Recombination

If we use a hydrogenic approximation to the cross-section for radiative recombination, then for a Maxwellian electron gas with temperature T , the emission spectrum due to captures into the state n of an ion Z, z is given by (Elwert 1954; Tucker and Gould 1966; Culhane 1969)

$$\begin{aligned} \frac{dE_{RR,Z,z}}{dt dV d\lambda}(T) &= \frac{dP_{RR,Z,z}}{d\lambda}(T) \\ &= \frac{6.52 \times 10^{-23}}{\lambda^2 T_6^{3/2}} N_e N_H X_{Z,z,n}(T) \exp(-144/\lambda T_6) \text{ ergs (cm}^3 \text{ sec } \text{\AA})^{-1} \\ &\quad (\lambda < 12400/I_{Z,z,n}), \\ &= 0 \quad (\lambda > 12400/I_{Z,z,n}), \end{aligned} \quad (8)$$

where λ is in angstroms, $I_{Z,z,n}$ is the ionization potential of the state n in electron volts, and

$$X_{Z,z,n}(T) = (N_{Z,z+1}/N_Z)(N_z/N_H)(\bar{s}/2n^2)n(I_{Z,z,n}/I_H)^2 \exp(0.0116I_{Z,z,n}/T_6). \quad (9)$$

Here $(\bar{s}/2n^2)$ is the incompletely fraction of shell n , and we have set the recombination Gaunt factor equal to unity. To obtain the spectrum of a plasma consisting of a mixture of ions Z, z , equation (8) must be summed over all ions and all levels n for which $I_{Z,z,n} > 12400/\lambda$. In performing this sum, we included sixty-four terms $X_{Z,z,n}$ which consisted of the five or six lowest levels for the more abundant species and the one or two lowest levels for the less abundant species. At any given temperature and wavelength only a few terms (< 10) in the sum contributed appreciably to the spectrum.

iii) Two-Photon Decay of the 2S States of Hydrogenic and Heliumlike Ions

Since the excitation rates of the metastable 2S states of hydrogenic and heliumlike ions are about one-third the rates for excitation of the 2P states (Beigman *et al.* 1970), the energy emitted in the two-photon process will be about a third of the energy emitted in the 2P-1S resonance transitions of these ions, unless collisional or single-photon processes are more efficient in depopulating the 2S state.

For hydrogenic ions, the two-photon transition probability is $A(2S-1S) \approx 8Z^6 \text{ sec}^{-1}$ (Spitzer and Greenstein 1951; Shapiro and Breit 1959). By comparison, single-photon processes are negligible. The most important collisional-depopulation process is proton excitation to the 2P state, which for coronal conditions ($n_H \sim 10^8 \text{ cm}^{-3}$; $T_6 \sim 1$) is completely negligible for $Z \geq 6$ (cf. Seaton 1955). The shape of the two-photon continuum has been computed for hydrogen by Spitzer and Greenstein (1951). It extends from the frequency $\nu = 0$ to $\nu = \nu_T = E(2S)/\hbar$, is symmetric about the central frequency $\frac{1}{2}\nu_T$, and has a maximum at $\frac{1}{2}\nu_T$. To a good approximation the spectral shape may be approximated by the function $H(\nu/\nu_T) = (\nu/\nu_T)(1 - \nu/\nu_T)$. If we assume that this spectral

shape applies to all hydrogenic ions, then the energy emitted per cm^3 per second per angstrom as a result of the two-photon decay of the $2S$ state of the ion $Z, Z - 1$ is given by

$$\frac{dP_{2\gamma, Z, Z-1}}{d\lambda}(T) = \frac{4P_{L, Z, Z-1}(2P - 1S)}{\lambda} \left(\frac{\lambda_T}{\lambda}\right)^3 \left(1 - \frac{\lambda_T}{\lambda}\right), \quad (10)$$

where $\lambda_T = c/v_T$ and $P_{L, Z, Z-1}$ is the power per cm^3 in the $L\alpha$ line of the ion $Z, Z - 1$.

In the case of heliumlike ions the metastable states 2^1S and 2^3S must be considered separately. Two-photon decay of 2^3S is unimportant, since the 2^3S state can decay through a single-photon magnetic-dipole transition which has a much larger probability than the two-photon process (Griem 1970; Gabriel and Jordan 1970).

The results for the 2^1S state are very similar to those for hydrogenic ions. The spectrum is roughly the same, and the transition probability is asymptotically equal to $16(Z - 1)^6$, or twice the two-photon-decay rate of the hydrogenic $2S$ state with nuclear charge $Z - 1$ (Drake, Victor, and Dalgarno 1969). Thus, collisional depopulation is unimportant for coronal conditions, and the intensity due to the two-photon continuum is proportional to the rate of excitation of the 2^1S from the ground state. The probability of exciting the 2^1S state is about one-third the probability of exciting the 2^3P , 2^1P , and 2^3S states, so that the intensity of the 2^1S two-photon continuum can be computed to a good approximation by using equation (10) with $P_{L, Z, Z-1}(2P - 1S, T)$ replaced by $P_{L, Z, Z-2}(2^3P - 1^1S, T) + P_{L, Z, Z-2}(2^1P - 1^1S, T) + P_{L, Z, Z-2}(2^3S - 1^1S, T)$.

III. RESULTS

The results of the calculation are presented in Tables 2 and 3, and in Figures 1–3. In Table 2 we list $-\log_{10} P_{L, Z, z}^{\text{ex}}(nn', T)/N_e^2$, the negative logarithm of the power in the lines, as a function of temperature. The lines are listed according to ionic species and wavelengths. The corresponding transition can be found in Table 1. In Table 2 the ions were specified by arabic rather than roman numerals to save space. The cutoffs in the table were determined by the availability of ionization-equilibrium calculations. This explains why the numbers for calcium ions cut off at 10^7 °K in every case. In the future we hope to extend the ionization-equilibrium calculations in order to eliminate such artificial cutoffs. The numbers in Table 1 refer only to line emission resulting from electron collisional excitation. Equations (4) and (6) can be used to obtain an estimate of the line emission produced as a result of K -shell excitation and dielectronic recombination.

To facilitate computation of radiative-recombination spectra, we have tabulated in Table 3 the recombination sum $S = \sum X_{Z, z, n}(\lambda, T)/T_6$ (see eq. [9]) as a function of wavelength and temperature. Only the values at the edges are given, since between the edges the sum is constant. Note that the ratio of S to the bremsstrahlung Gaunt factor g_B is equal to the ratio of recombination radiation to bremsstrahlung radiation. Since $g_B \approx 1-1.3$ for most wavelengths and temperatures of interest, S gives the ratio of recombination to bremsstrahlung emission within a factor of 2. From the numbers given in Table 3, we see that for a given temperature T_6 , recombination dominates bremsstrahlung at wavelengths below about $600/T_6$ Å. For wavelengths larger than this value, bremsstrahlung dominates.

In Figure 1 we have plotted the spectrum of a coronal plasma for several different temperatures. A resolution of 0.5 Å was assumed, and some prominent lines are labeled according to the ion and wavelength. The smooth curves show the contribution of the various continuum processes. The processes of bremsstrahlung (B), radiative recombination (RR), and two-photon emission (2γ) are shown. The dashed line represents the total continuum emission (C). The spectrum is expressed in units of $\text{ergs cm}^3 \text{ sec}^{-1} \text{ Å}^{-1}$, so that multiplication by the emission integral $\int N_e^2 dV$ gives the power emitted per angstrom.

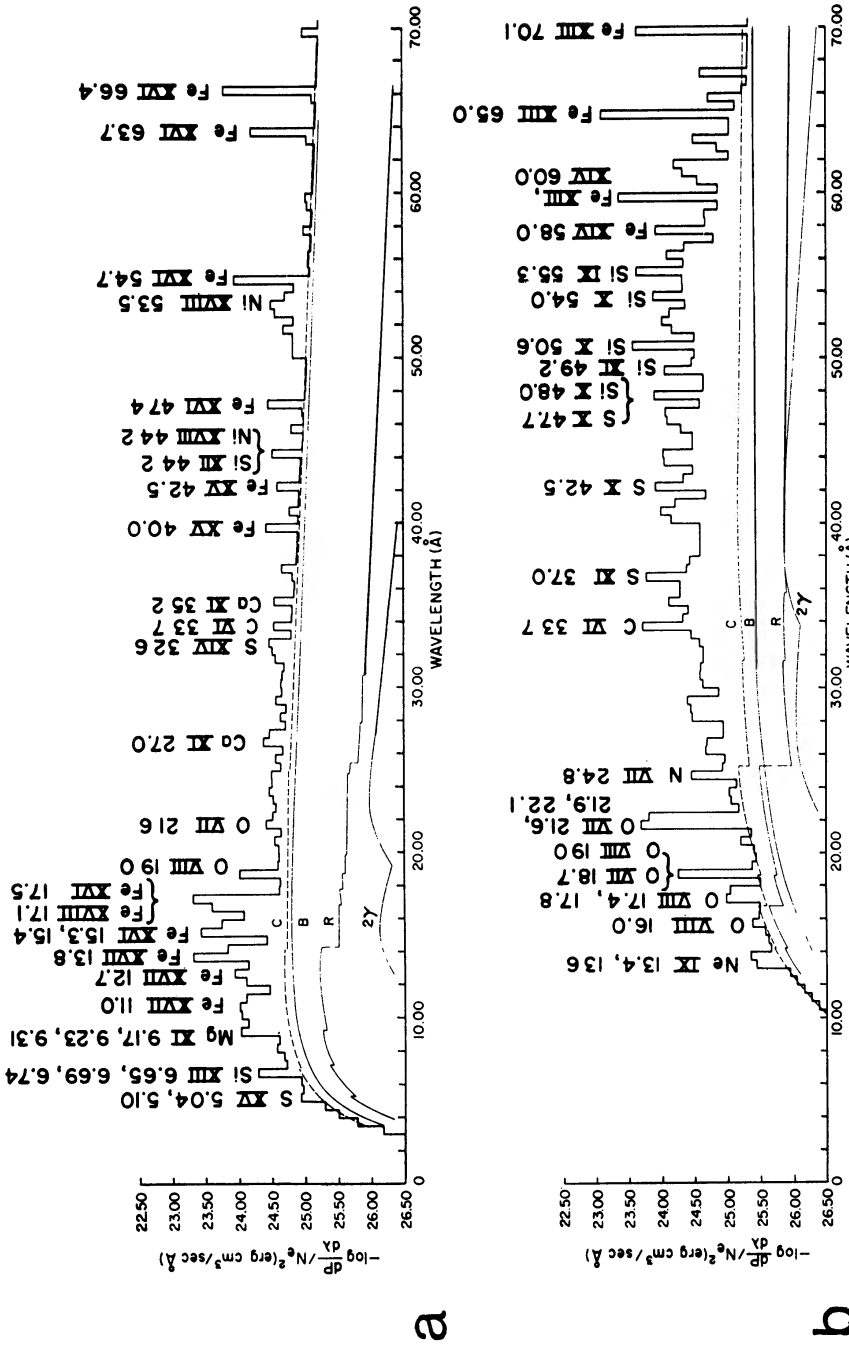


FIG. 1.—The spectrum of a coronal plasma, if a resolution of 0.5 Å is assumed. Some prominent lines are labeled according to ion and wavelength. The continuum processes of bremsstrahlung (B), radiative recombination (RR), and two-photon emission (2γ) are shown. Dashed line represents the total continuum emission (C). (a) $T = 5 \times 10^6$ K; (b) $T = 1.6 \times 10^6$ K; (c) $T = 1.6 \times 10^7$ K; (d) $T = 5 \times 10^7$ K.

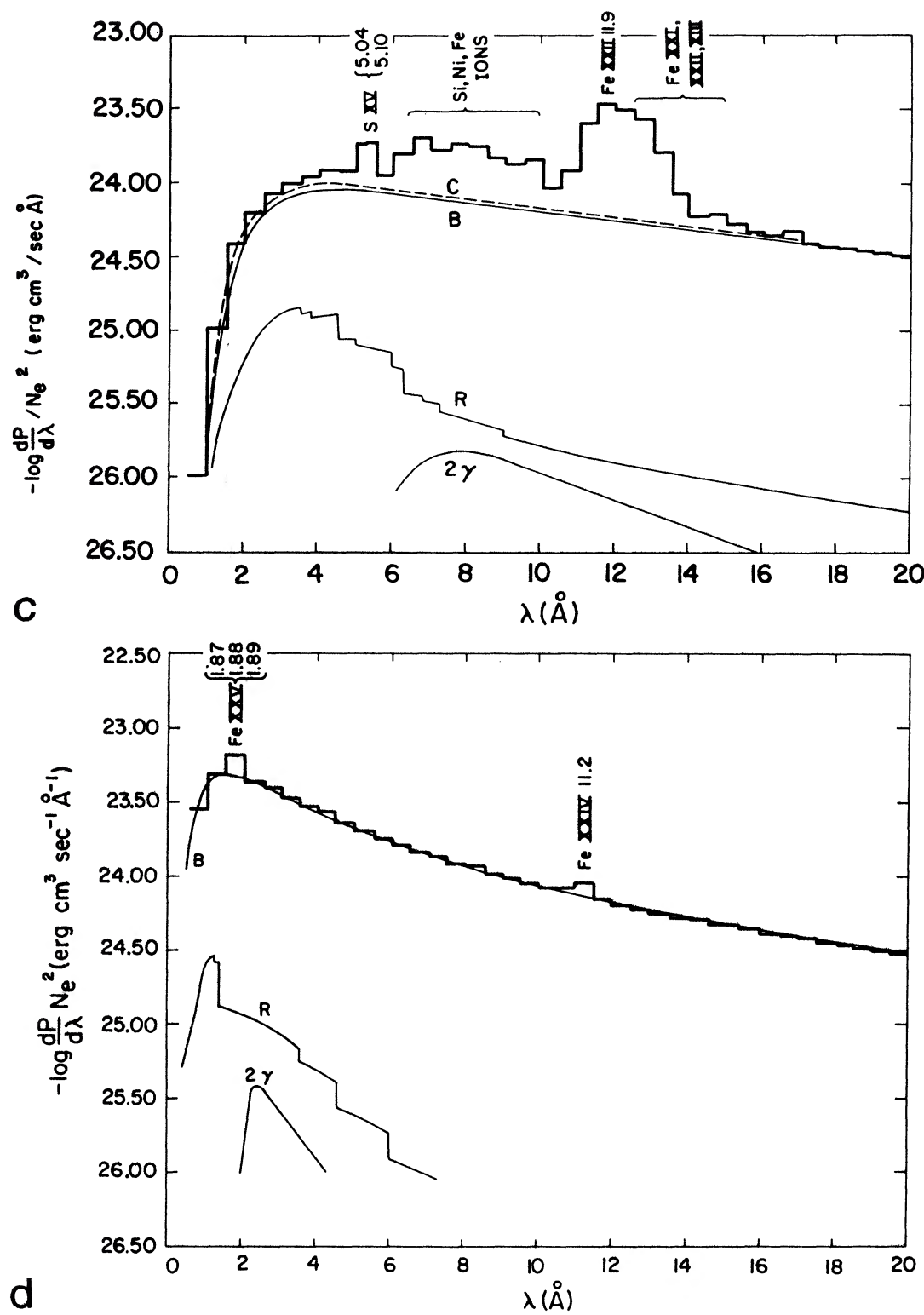


FIG 1—Continued

TABLE 2
LOG POWER IN LINES (ergs cm⁻³ s⁻¹) AS A FUNCTION OF TEMPERATURE (° K)

	λ	5.8	6.2	6.4	6.6	6.8	7.0	7.3	7.6	8.0	Log T =
NIXXVIII	1.21	31.52	28.42	27.01	
NIXXVIII	1.24	31.32	28.25	26.87	
NIXXVII	1.29	34.28	28.15	26.83	26.81	
NIXXVII	1.30	34.37	28.25	26.93	26.92	
NIXXVIII	1.31	30.88	27.88	26.54	
NIXXVII	1.37	33.76	27.76	26.51	26.53	
FeXXVI	1.40	29.76	27.20	26.06	
FeXXVI	1.43	29.58	27.05	25.92	
FeXXV	1.50	30.86	26.69	25.67	25.79	
FeXXV	1.51	30.87	26.75	25.75	25.89	
FeXXVI	1.51	29.17	26.69	25.60	
NIXXVIII	1.55	29.80	26.98	25.75	
FeXXV	1.59	30.29	26.28	25.34	25.51	
NIXXVII	1.60	32.43	26.76	25.68	25.80	
NIXXVII	1.61	32.63	26.97	25.89	26.01	
NIXXVII	1.62	32.71	27.07	25.99	26.12	
FeXXVI	1.79	28.12	25.81	24.81	
FeXXV	1.87	29.05	25.32	24.52	24.78	
FeXXV	1.88	29.27	25.55	24.76	25.02	
FeXXV	1.89	29.32	25.61	24.82	25.08	
CaXX	2.30	
CaXX	2.40	
CaXIX	2.50	
CaXX	2.54	
CaXIX	2.60	
CaXIX	2.70	
CaXX	3.02	
CaXIX	3.18	
CaXIX	3.20	
CaXIX	3.22	
SXVI	3.70	32.99	29.82	27.92	26.60	26.78	27.54	
SXVI	3.78	32.78	29.64	27.76	26.46	26.65	27.41	
SXVI	3.99	32.26	29.20	27.38	26.12	26.33	27.10	
SXV	4.01	37.64	31.12	28.37	26.99	26.22	25.98	26.86	28.50	
SXV	4.10	37.52	31.09	28.39	27.05	26.29	26.07	26.96	28.60	
SXV	4.30	36.77	30.50	27.91	26.63	25.91	25.73	26.64	28.29	
SXVI	4.73	30.95	28.12	26.44	25.30	25.57	26.38	
SIXIV	4.83	33.90	30.96	27.54	26.25	26.10	26.62	
SIXIV	4.95	34.02	31.08	27.66	26.38	26.23	26.74	
SXV	5.04	34.75	28.96	26.67	25.58	24.98	24.90	25.86	27.55	
SXV	5.07	35.11	29.34	27.05	25.97	25.38	25.30	26.26	27.94	
SXV	5.10	34.83	29.07	26.31	25.73	25.14	25.07	26.04	27.72	
SIXIV	5.22	33.51	30.60	27.20	25.93	25.79	26.31	
SIXIII	5.29	39.67	32.03	28.61	26.93	25.99	25.71	26.56	
SIXIII	5.40	39.78	32.14	28.72	27.04	26.10	25.82	26.67	
SIXIII	5.68	38.94	31.50	28.21	26.62	25.73	25.48	26.36	

TABLE 2—Continued

NiXXVI	6.14	29.13	25.92	26.19	27.43
SiXIV	6.18	31.87	29.30	26.12	24.98	24.95	25.53
MgXII	6.60	30.86	28.05	26.55	26.25	26.69
NiXXIV	6.62	30.43	26.95	25.68	27.47	30.46
SiXIII	6.65	36.58	29.74	26.83	25.47	24.73	24.57	25.53
SiXIII	6.69	36.97	30.15	27.25	25.90	25.17	25.01	25.98
MgXII	6.70	30.98	28.17	26.68	26.37	26.82
SiXIII	6.74	36.63	29.83	26.94	25.60	24.87	24.71	25.68
NiXXV	6.76	28.48	26.30	27.35	29.46
NiXXIII	6.94	28.70	26.31	25.95	28.51
NiXXVI	7.10	29.05	25.92	26.22	27.48
MgXII	7.11	30.33	27.61	26.16	25.89	26.36
FeXXIV	7.21	30.43	26.58	24.95	25.29	26.58
NiXXII	7.26	31.20	27.89	25.88	26.46	29.75
MgXI	7.30	32.84	29.29	27.42	26.33	25.95	26.42
FeXXI	7.40	26.84	25.14	26.22
MgXI	7.47	33.04	29.47	27.57	26.46	26.07	26.54
NiXXV	7.50	28.45	26.30	27.37	29.49
NiXXI	7.60	29.08	26.78	25.58	27.08
NiXXIII	7.70	28.70	26.30	25.94	28.50
MgXI	7.86	32.26	28.85	27.06	26.02	25.67	26.16
FeXXII	7.89	27.23	24.72	24.93	26.72
FeXXI	7.90	26.87	25.15	26.21
NiXXIV	7.94	30.35	26.91	25.68	27.49	30.49
FeXXI	8.00	26.60	24.91	25.99
FeXXIII	8.00	29.22	25.95	25.28	26.35	28.49
NiIXX	8.10	27.58	26.17	25.61	25.66	28.86
NiXX	8.25	29.84	27.29	25.84	25.30	27.65
NiIXX	8.30	27.91	26.53	25.99	26.05	29.26
FeXXI	8.30	26.40	24.71	25.79
FeXXIV	8.35	30.31	26.52	24.96	25.32	26.63
MgXII	8.42	29.07	26.54	25.23	25.03	25.57
FeXIX	8.60	27.79	25.70	25.22	27.82
NiXXII	8.60	31.04	27.80	25.85	26.47	29.77
NiXXI	8.60	28.92	26.69	25.54	27.09
NiXXI	8.83	28.97	26.72	25.55	27.08
FeXXIII	8.86	29.16	25.92	25.28	26.37	28.52
FeXXI	8.95	26.53	24.88	26.00
NiIXX	9.00	27.31	26.01	25.53	25.63	28.86
NiIXX	9.10	27.29	26.00	25.53	25.63	28.86
FeXVIII	9.15	33.98	28.50	26.41	25.26	25.45	28.90
MgXI	9.17	30.45	27.45	25.92	25.04	24.80	25.35
FeXX	9.20	29.03	26.16	25.09	26.89
NiXXVI	9.20	28.85	25.81	26.16	27.44
MgXI	9.23	30.92	27.93	26.41	25.54	25.30	25.86
NiXXII	9.25	30.91	27.78	25.89	26.57	29.90
MgXI	9.31	30.47	27.51	26.00	25.13	24.90	25.46
NiXXIV	9.32	30.25	26.92	25.79	27.65	30.68
NiXXIII	9.35	28.64	26.36	26.11	28.73
FeXXII	9.45	27.17	24.70	24.93	26.74

TABLE 2--Continued

FeXIX	9.50	27.67	25.64	25.20	27.83
NiXXV	9.50	28.25	26.19	27.31	29.46
NeX	9.50	31.03	28.00	26.46	26.26	26.58	27.17
NiXXVI	9.52	28.76	25.72	26.07	27.35
FeXX	9.60	29.03	26.16	25.09	26.89
NiXXIII	9.60	35.01	29.82	27.07	28.44
NiXXII	9.65	30.53	27.43	25.56	26.25	29.59
FeXX	9.70	28.98	26.13	25.08	26.90
FeXIX	9.70	27.37	25.34	24.90	27.53
FeXIX	9.70	27.60	25.60	25.19	27.84
NeX	9.70	31.16	28.12	26.59	26.39	26.70	27.30
NiXXVI	9.70	28.89	25.86	26.21	27.50
NiXXIII	9.70	28.48	26.16	25.87	28.46
NiXXI	9.70	28.80	26.49	25.29	26.80
NiXXV	9.75	28.28	26.21	27.32	29.46
FeXXI	9.81	26.46	24.73	25.79
NiXXI	9.86	28.87	26.66	25.52	27.07
FeXVII	9.90	29.91	26.04	24.96	24.64	25.44	29.64
FeXIX	10.00	27.60	25.60	25.19	27.84
NiXXIX	10.00	27.49	26.29	25.87	26.00	29.27
NiXXV	10.00	28.27	26.21	27.32	29.47
NiXXIV	10.00	29.91	26.61	25.49	27.37	30.40
NiXXIX	10.00	27.01	25.81	25.39	25.53	28.80
NiXXII	10.04	30.48	27.41	25.55	26.26	29.60
FeXVII	10.10	30.16	26.30	25.24	24.93	25.74	29.95
FeXX	10.20	29.09	26.22	25.15	26.95
FeXVIII	10.20	33.38	28.05	26.06	24.97	25.19	28.68
NeX	10.20	30.50	27.54	26.05	25.89	26.22	26.83
NiXXV	10.20	28.27	26.21	27.33	29.48
NiXXIX	10.30	26.19	25.10	24.75	24.93	28.24
FeXIX	10.40	27.30	25.30	24.89	27.54
FeXVIII	10.40	33.26	27.93	25.93	24.85	25.07	28.55
NiXXIV	10.40	30.49	27.20	26.10	27.98	31.02
NiXX	10.40	29.92	27.46	26.08	25.57	27.95
FeXX	10.50	28.98	26.13	25.08	26.90
NiXXIII	10.60	28.64	26.35	26.09	28.70
FeXX	10.70	29.03	26.19	25.14	26.96
FeXVIII	10.70	33.98	28.50	26.41	25.26	25.45	28.90
NiXXIII	10.70	28.55	26.33	26.13	28.77
NiXXII	10.70	30.71	27.55	25.63	26.29	29.61
FeXIX	10.80	27.60	25.60	25.19	27.84
FeXXIV	10.80	30.03	26.34	24.86	25.26	26.60
FeXIX	10.80	26.73	24.83	24.48	27.18
NiXX	10.80	29.62	27.16	25.78	25.27	27.65
NeIX	10.80	29.58	27.56	26.38	26.06	26.65	27.57
FeXVIII	10.90	33.93	28.44	26.35	25.21	25.39	28.84
FeXVIII	10.90	33.42	28.17	26.23	25.17	25.42	28.92
FeXVII	11.00	29.57	25.84	24.85	24.58	25.42	29.66
NiXXIX	11.00	26.91	25.79	25.42	25.59	28.89
NeIX	11.00	29.69	27.67	26.48	26.17	26.76	27.68

TABLE 2—Continued

NiXXIV	11.00	30.03	26.69	25.54	27.40	30.42
FeXIX	11.10	27.60	25.60	25.19	27.84
FeXVII	11.10	29.55	25.82	24.84	24.58	25.42	29.66
FeXXIV	11.20	29.75	26.06	24.58	24.99	26.32
FeXXIII	11.20	28.90	25.75	25.19	26.32	28.50
FeXXIV	11.40	30.06	26.38	24.90	25.31	26.65
FeXXIII	11.50	28.94	25.78	25.21	26.33	28.51
FeXXII	11.50	27.12	24.74	25.06	26.91
NeIX	11.60	29.06	27.15	26.03	25.76	26.38	27.32
NiXXI	11.60	29.29	27.15	26.06	27.65
NiXX	11.60	28.86	26.63	25.39	24.97	27.44
NiXXIV	11.70	30.22	26.88	25.74	27.61	30.63
NiXXII	11.70	30.68	27.65	25.82	26.55	29.91
FeXXIII	11.80	28.93	25.77	25.21	26.34	28.51
NiXXI	11.80	29.05	26.78	25.60	27.12
FeXXII	11.90	26.80	24.44	24.78	26.64
CaXVIII	12.00	26.66	25.71
FeXXI	12.00	26.11	24.52	25.68
FeXXIII	12.00	28.92	25.77	25.21	26.34	28.52
NiXXII	12.00	30.39	27.78	25.90	26.59	29.93
FeXVIII	12.20	32.85	27.74	25.89	24.89	25.17	28.71
NeX	12.20	29.16	26.43	25.09	25.01	25.40	26.06
FeXXI	12.30	25.92	24.29	25.42
FeXVIII	12.40	32.73	27.62	25.76	24.77	25.05	28.58
FeXXII	12.40	27.38	25.03	25.38	27.24
NiXIX	12.40	28.06	27.04	26.72	26.93	30.25
NiXX	12.60	29.06	26.82	25.57	25.15	27.61
NiXIX	12.60	26.38	25.38	25.08	25.29	28.62
FeXXI	12.70	25.45	23.88	25.07
FeXVII	12.70	29.02	25.52	24.68	24.51	25.40	29.69
FeXX	12.70	28.30	25.53	24.53	26.39
NiXIX	12.80	27.96	26.96	26.66	26.88	30.21
FeXXI	12.90	26.09	24.49	25.65
NiXX	12.90	28.58	26.41	25.21	24.82	27.30
FeXVIII	13.00	33.36	28.11	26.17	25.12	25.36	28.86
CaXVII	13.00	26.53	26.26
CaXVI	13.00	28.31	26.13	26.57
FeXXII	13.10	26.89	24.50	24.81	26.66
NiXX	13.10	28.96	26.80	25.60	25.22	27.70
FeXX	13.40	27.93	25.19	24.20	26.08
FeXVIII	13.40	32.78	27.57	25.65	24.61	24.86	28.37
NeIX	13.40	27.61	25.97	25.02	24.86	25.54	26.52
FeXXI	13.50	26.04	24.50	25.71
NeIX	13.60	28.11	26.50	25.57	25.41	26.11	27.09
NiXVII	13.60	29.20	25.97	26.07	26.37	27.34
FeXVIII	13.70	33.42	28.17	26.23	25.17	25.42	28.92
NeIX	13.70	27.60	26.00	25.08	24.93	25.62	26.61
NiXVIII	13.70	30.20	25.91	25.21	25.04	25.51	29.25
NiXIX	13.80	26.14	25.20	24.94	25.18	28.53
FeXVII	13.80	28.12	24.66	23.84	23.68	24.59	28.89

TABLE 2--Continued

FeXXII	13.90	27.09	24.71	25.02	26.87
FeXIX	14.00	26.61	24.63	24.22	26.88
FeXIX	14.20	26.69	24.81	24.46	27.17
NiXIX	14.30	26.04	25.11	24.86	25.10	28.46
FeXVIII	14.40	31.56	26.64	24.90	23.97	24.30	27.87
FeXX	14.40	27.89	25.18	24.20	26.09
NiXVII	14.40	29.50	26.25	26.33	26.63	27.60
NiXVIII	14.50	30.54	26.22	25.51	25.33	25.79	29.52
FeXX	14.70	28.08	25.29	24.27	26.12
OVIII	14.80	29.54	26.66	25.46	25.48	25.84	26.24
FeXIX	15.00	27.15	25.32	25.02	27.76
CaXVIII	15.00	26.63	25.71
FeXVII	15.00	29.86	26.49	25.73	25.60	26.53	30.84
CaXVI	15.00	28.26	26.11	26.57
CaXV	15.10	27.49	25.97	27.04
FeXX	15.20	28.43	25.75	24.80	26.71
FeXIX	15.20	26.83	24.89	24.52	27.20
OVIII	15.20	29.67	26.78	25.58	25.61	25.97	26.37
FeXVII	15.30	28.32	24.96	24.22	24.10	25.03	29.35
FeXVI	15.40	33.12	27.83	24.79	24.26	24.40	25.62
FeXVIII	15.40	31.76	26.83	25.09	24.16	24.48	28.05
FeXVII	15.50	29.89	26.54	25.80	25.69	26.63	30.95
OVIII	16.00	29.04	26.22	25.08	25.13	25.51	25.92
CaXVII	16.00	26.51	26.26
FeXVIII	16.00	31.22	26.37	24.69	23.79	24.14	27.73
FeXVIII	16.20	31.60	26.77	25.09	24.20	24.55	28.14
FeXX	16.30	28.42	25.75	24.80	26.71
CaXV	16.30	27.50	25.98	27.04
FeXX	16.60	28.29	25.55	24.56	26.43
FeXVII	16.80	28.03	24.76	24.06	23.98	24.93	29.27
FeXV	17.00	30.89	26.14	25.16	25.02	25.66	27.30
FeXVI	17.10	33.09	27.97	25.04	24.57	24.75	26.00
FeXVII	17.10	27.93	24.67	23.99	23.91	24.87	29.20
CaXIV	17.20	26.53	25.64	27.21
OVII	17.40	26.49	25.42	25.32	26.05	26.98	27.84
FeXVI	17.50	32.34	27.36	24.51	24.10	24.32	25.59
OVII	17.80	26.60	25.52	25.43	26.16	27.08	27.95
CaXVIII	18.00	26.60	25.73
FeXV	18.00	31.20	26.43	25.42	25.28	25.91	27.55
OVII	18.70	25.76	24.74	24.69	25.44	26.38	27.26
OVIII	19.00	27.70	25.12	24.11	24.26	24.69	25.14
CaXIII	19.20	27.51	26.06	25.87	27.93
NVII	19.40	28.00	26.38	26.28	26.64	27.04	27.46
CaXVI	19.50	27.37	25.31	25.83
NVII	19.80	28.12	26.51	26.40	26.76	27.17	27.58
CaXVIII	20.00	26.12	25.25
CaXV	20.40	27.47	26.05	27.17
CaXIV	20.40	26.49	25.63	27.22
CaXII	20.80	28.76	26.83	25.88	26.41
NVII	20.90	27.53	25.98	25.91	26.29	26.72	27.14

TABLE 2—Continued

CaXV	20.90	26.63	25.22	26.36
CaXVIII	21.00	26.60	25.73
SXIII	21.00	31.30	26.79	25.21	25.83	26.65	27.32
CaXV	21.10	27.06	25.60	26.71
CaXIII	21.60	27.43	26.03	25.87	27.95
OVII	21.60	24.96	24.11	24.15	24.98	25.96	26.86
OVII	21.80	25.55	24.71	24.76	25.59	26.57	27.48
SXIV	22.00	28.36	25.81	25.71	25.94	26.10
CaXVII	22.00	25.84	25.63
CaXIV	22.00	26.71	25.90	27.51
OVII	22.10	24.96	24.14	24.20	25.04	26.03	26.93
CaXIII	22.20	27.45	26.04	25.87	27.95
CaXII	23.00	28.62	26.76	25.85	26.41
CaXV	23.20	26.95	25.54	26.68
NVI	23.30	26.42	26.23	26.84	27.80	28.67	29.59
NVI	23.80	26.54	26.35	26.96	27.93	28.79	29.72
SXII	23.90	28.70	25.56	24.81	26.09	27.46	28.62
CaXII	23.90	28.62	26.76	25.85	26.41
CaXI	24.00	26.70	25.67	25.28	26.27
SXIV	24.20	28.24	25.76	25.69	25.94	26.11
CaXIII	24.50	27.07	25.60	25.40	27.45
NVII	24.80	26.34	24.96	25.01	25.46	25.92	26.37
NVI	25.00	26.07	25.93	26.57	27.55	28.43	29.36
CaXIV	25.00	25.78	24.99	26.61
CaXIV	25.80	26.26	25.44	27.04
CaXIII	25.80	27.12	25.72	25.57	27.66
SXIII	26.00	31.18	26.72	25.17	25.82	26.65	27.33
CVI	26.40	25.65	25.41	25.77	26.18	26.60	27.01
CaXI	26.70	26.60	25.63	25.26	26.27
SXI	26.80	27.10	25.16	25.28	27.15	29.03
CaXI	27.00	26.42	25.47	25.12	26.14
CVI	27.00	25.77	25.54	25.90	26.31	26.73	27.14
CaXII	27.30	27.64	25.87	25.02	25.62
CaXIV	27.80	26.36	25.59	27.23
CVI	28.50	25.22	25.04	25.43	25.35	26.28	26.70
CaXIV	28.50	26.56	25.76	27.38
SXII	28.70	28.54	25.47	24.77	26.08	27.46	28.64
SXI	28.80	27.13	25.18	25.29	27.15	29.02
NVI	28.80	25.03	25.01	25.73	26.76	27.67	28.62
NVI	29.10	25.76	25.75	26.47	27.50	28.42	29.37
CaXII	29.20	27.86	26.14	25.31	25.92
CaXIII	29.40	27.53	26.18	26.06	28.17
NVI	29.50	24.94	24.94	25.66	26.70	27.62	28.57
SXII	29.80	28.33	25.45	25.15	25.56	25.90	26.47
CaXIII	29.80	27.39	25.96	25.79	27.86
SXIV	30.20	28.02	25.65	25.66	25.96	26.16
SXIII	31.00	30.72	26.45	25.03	25.75	26.63	27.34
CaXI	31.20	26.43	25.55	25.24	26.28
SX	31.40	25.72	24.84	25.70	28.16
CaXII	32.50	28.16	26.48	25.69	26.32

TABLE 2—*Continued*

SXIV	32.60	27.62	25.25	25.26	25.56	25.76
SIXI	32.70	26.52	24.77	25.26	26.28	27.17
CaXII	32.70	27.33	25.65	24.85	25.48
SIXII	32.80	28.19	25.38	25.11	25.55	25.92	26.49
NIXVII	32.80	27.77	25.18	25.67	26.24	27.36
CV	32.80	25.42	26.07
SXII	33.30	28.33	25.46	24.88	26.27	27.70	28.91
CV	33.40	25.51	26.18
CVI	33.70	24.17	24.10	24.57	25.05	25.51	25.95
SXIV	33.80	28.00	25.64	25.66	25.96	26.16
SIX	34.20	25.17	24.38	25.59	27.21
SXIII	35.00	30.45	26.14	24.68	25.39	26.26	26.95
CV	35.10	25.10	25.80
CaXI	35.20	25.89	25.07	24.30	25.87
SXII	35.40	27.88	25.00	24.42	25.81	27.24	28.45
SIXI	36.20	26.44	24.72	25.24	26.28	27.18
SXI	36.20	26.78	25.03	25.28	27.23	29.15
SIX	36.80	25.12	25.24	26.72
SXIII	37.00	30.69	26.41	24.98	25.69	26.57	27.27
SXI	37.00	25.93	24.20	24.46	26.42	28.35
NIXVIII	37.00	28.77	25.27	25.07	25.22	25.89	29.79
FeXVI	37.10	31.95	27.71	25.33	25.21	25.61	27.00
SX	37.20	25.58	24.77	25.67	28.15
SXI	37.30	26.50	24.67	24.87	26.79	28.69
SXII	37.80	28.35	25.52	24.96	26.37	27.82	29.03
SIXX	38.00	25.46	25.61	27.53
SXII	39.80	27.99	25.09	24.49	25.87	27.30	28.50
FeXVI	40.00	31.53	27.27	24.88	24.75	25.15	26.53
SIXX	40.00	24.71	24.88	26.82
SX	40.20	25.66	24.95	25.91	28.43
CV	40.30	24.10	24.89
CV	40.70	25.11	25.90
SIXII	40.90	27.86	25.19	25.01	25.51	25.90	26.50
SIX	41.00	25.07	24.33	25.57	27.21
SXI	41.00	26.21	24.50	24.77	26.73	28.67
FeXV	41.00	28.80	24.93	24.50	24.72	25.58	27.36
CV	41.50	24.05	24.85
SIX	41.50	25.11	25.23	26.72
SVIII	41.60	25.39	26.18	28.22
NIXVII	42.20	27.58	25.12	25.70	26.32	27.48
SXII	42.40	28.28	25.39	24.80	26.18	27.62	28.82
FeXVI	42.50	31.81	27.58	25.21	25.10	25.51	26.89
SX	42.50	24.99	24.31	25.28	27.82
SIX	42.60	25.04	25.20	26.71
MgX	43.00	25.50	25.41	25.86	26.08	26.54
SIXX	43.00	25.01	25.14	27.05
NIXVI	43.00	32.10	27.05	25.27	26.36	27.27	28.89
NIXVIII	43.70	29.28	25.82	25.64	25.80	26.48	30.39
SIXI	43.80	26.13	24.55	25.16	26.25	27.19
NIXVI	44.00	32.46	27.41	25.64	26.73	27.64	29.27

TABLE 2—*Continued*

SIXII	44.20	27.51	24.84	24.66	25.15	25.55	26.15
SIXIX	44.20	24.60	24.83	26.80
NIXVIII	44.20	28.96	25.46	25.27	25.42	26.09	30.00
NIXV	45.00	30.39	26.45	25.51	27.25	28.54
NIXVI	45.50	32.38	27.19	25.32	26.35	27.22	28.83
SIXII	45.60	27.78	25.12	24.95	25.45	25.85	26.46
NIXVII	45.60	28.03	25.55	26.12	26.72	27.88
SX	45.80	24.95	24.29	25.28	27.82
S VIII	46.00	25.29	26.14	28.21
SIXI	46.30	26.15	24.52	25.10	26.17	27.09
NIXV	46.60	30.48	26.39	25.36	27.04	28.29
Mg IX	47.00	24.96	25.72	26.81	27.72
SX	47.00	25.26	24.52	25.45	27.96
SIX	47.00	24.69	24.78	26.25
NIXVI	47.00	31.88	26.86	25.10	26.21	27.12	28.76
Mg X	47.30	25.39	25.36	25.84	26.09	26.56
Fe XVI	47.40	31.55	27.28	24.88	24.75	25.15	26.53
S VIII	47.60	25.21	26.14	28.69
S VIII	47.70	25.52	26.37	28.88
SX	47.70	25.48	24.86	25.87	28.43
S VIII	47.80	25.29	26.14	28.21
SIX	48.00	25.01	24.41	25.74	27.43
SIXI	49.20	26.09	24.49	25.09	26.17	27.11
SIX	49.30	24.68	24.87	26.40
SVII	50.00	25.28	26.69
NIXV	50.00	29.71	25.81	24.91	26.66	27.97
SIX	50.60	24.51	23.93	25.29	26.98
SX	50.60	25.45	24.85	25.87	28.43
NIXVIII	51.70	29.13	25.68	25.52	25.68	26.37	30.28
Mg IX	52.00	24.87	25.68	26.81	27.73
SX	52.00	25.48	24.79	25.76	28.29
SIXI	52.30	26.09	24.50	25.10	26.19	27.13
S VIII	52.40	25.33	26.29	28.86
S VIII	52.50	25.27	26.16	28.69
Fe XV	52.90	28.49	24.81	24.49	24.78	25.69	27.50
Mg VIII	53.50	24.54	26.09	27.78	29.15
NIXVIII	53.50	28.78	25.27	25.07	25.21	25.88	29.79
S VIII	53.80	25.29	26.27	28.85
Fe XV	53.90	28.96	25.25	24.91	25.18	26.09	27.89
SIX	54.00	25.01	24.46	25.83	27.54
SIX	54.00	24.55	24.86	26.88
NIXV	54.00	30.61	26.59	25.61	27.32	28.59
Fe XVI	54.20	30.88	26.80	24.53	24.48	24.92	26.33
S VIII	54.50	25.71	26.63	29.16
SVII	54.60	24.37	25.29	27.40
Fe XVI	54.70	30.59	26.48	24.18	24.11	24.55	25.95
SVII	54.90	25.23	26.67
SVII	55.00	25.08	26.53
NIXVI	55.00	32.44	27.33	25.51	26.58	27.48	29.10
SIX	55.30	23.69	24.03	26.07

TABLE 2—Continued

SiIX	55.70	24.21	24.46	26.45
NiXVI	55.70	32.32	27.38	25.67	26.30	27.74	29.39
FeXIV	56.00	26.92	24.24	24.70	25.44	26.90	29.21
NiXVII	56.00	28.01	25.63	26.26	26.90	28.08
FeXIV	56.20	27.29	24.61	25.07	25.81	27.26	29.58
SiX	56.30	25.04	25.30	26.87
SiVII	56.50	25.39	27.01
SiX	56.80	24.66	24.04	25.36	27.04
SiX	57.00	24.98	25.12	26.63
MgX	57.90	25.28	25.33	25.87	26.15	26.64
FeXIV	58.00	27.13	24.33	24.72	25.41	26.84	29.14
SVIII	58.50	24.62	25.58	27.72
SiVIII	58.90	24.58	25.60	28.20
FeXIII	59.00	25.82	24.05	25.24	26.38	28.40
NiXV	59.00	30.16	26.33	25.46	27.25	28.57
NiXVII	59.50	27.69	25.29	25.90	26.54	27.71
FeXIV	60.00	26.72	24.06	24.54	25.29	26.75	29.07
FeXIII	60.00	25.81	23.92	25.05	26.15	28.13
SiX	60.50	24.96	24.34	25.66	27.34
SVII	60.80	25.14	26.64
SiVIII	61.00	23.95	24.99	27.60
SiIX	61.20	24.44	24.73	26.75
SiIX	61.70	24.20	24.58	26.64
MgIX	62.80	24.74	25.63	26.80	27.75
MgX	63.30	24.90	24.95	25.48	25.76	26.25
MgVII	63.40	26.06	28.34
FeXVI	63.70	30.74	26.69	24.43	24.38	24.84	26.25
SiVII	64.00	25.31	26.98
MgVIII	64.30	24.42	26.04	27.79	29.18
SVIII	64.30	24.12	25.10	27.25
SVIII	65.00	24.93	25.93	28.09
FeXIII	65.00	25.15	23.42	24.63	25.79	27.81
SiVII	65.60	25.34	26.99
SiVIII	65.80	23.93	24.98	27.60
NeVIII	65.90	25.59	26.06	26.43	27.04
MgX	65.90	25.18	25.24	25.79	26.07	26.56
FeXVI	66.40	30.45	26.33	24.02	23.95	24.39	25.79
MgVII	66.80	25.12	27.41
MgIX	67.20	24.68	25.53	26.68	27.62
SiVIII	67.30	24.16	25.15	27.74
SiVIII	69.80	24.44	25.52	28.16
FeXIV	70.00	27.22	24.50	24.93	25.65	27.09	29.40
FeXIII	70.00	25.97	24.15	25.30	26.42	28.42
FeXV	70.00	28.84	25.26	25.01	25.34	26.28	28.10
FeXIV	71.00	27.20	24.61	25.12	25.39	27.37	29.70
MgVIII	71.70	24.85	26.49	28.25	29.66
MgVII	71.80	25.40	27.72
MgIX	72.30	24.64	25.52	26.68	27.63
SVII	72.40	24.63	26.19
SiVII	72.50	24.92	26.53

TABLE 2—Continued

MgVII	72.90	25.73	27.99
SIVIII	73.40	24.95	26.65
SIVIII	74.20	24.43	25.52	28.17
FeXV	74.50	28.54	24.92	24.65	24.97	25.89	27.72
NevIII	74.60	25.53	26.04	26.44	27.06
MgVIII	75.00	24.26	25.93	27.71	29.13
SIVIII	76.00	24.39	25.43	28.04
FeXIII	76.00	25.63	23.95	25.20	26.38	28.41
MgVIII	77.40	24.41	26.03	27.77	29.17
MgIX	77.70	24.64	25.54	26.72	27.68
SIVIII	79.50	25.36	27.10
MgVII	81.00	25.60	27.89

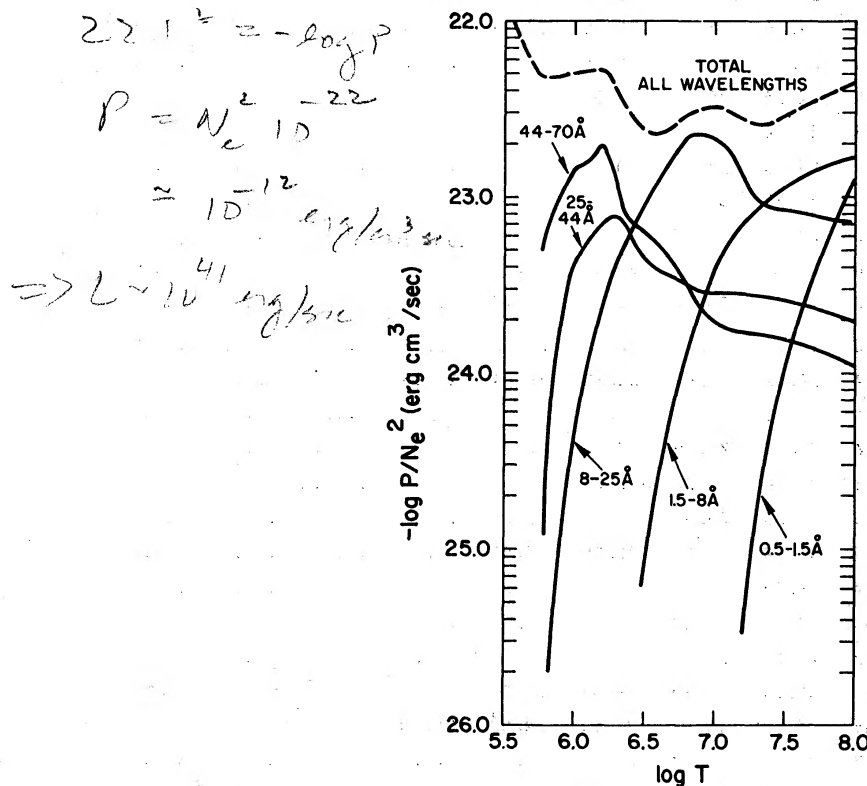


FIG. 2.—Power radiated in various wavelength bands as a function of temperature

These figures show the gradual shift from a line to a continuous spectrum and the concentration of the lines toward shorter wavelengths as the temperature increases.

In Figure 2 the power radiated in various wavelength bands is plotted as a function of temperature.

Finally, in Figure 3 the intensities of several of the strongest lines are plotted as a function of temperature.

TABLE 3
EDGES IN RECOMBINATION SUM S AS A FUNCTION OF
TEMPERATURE ($^{\circ}$ K) AND WAVELENGTH (Å)

λ	Ion	Log T =									
		6.0	6.2	6.4	6.6	6.8	7.0	7.2	7.4	7.6	8.0
2050.00	HeII	0.25	0.15	0.10	0.06	0.04	0.02	0.02	0.01	0.01
912.00	HI	0.37	0.23	0.14	0.09	0.06	0.04
225.00	OVI	2.01	1.21	0.74	0.46	0.28	0.18	0.11	0.07	0.04	0.02
141.00	CV	8.06	4.22	2.38	1.40	0.84	0.52	0.32	0.20	0.13	0.05
100.00	SiIX	8.18	4.33	2.43	1.43	0.86	0.53
93.20	FeX	8.37	4.40
86.70	FeXVI	8.47	4.42
74.20	NVII	8.52	4.45	2.46	1.44
71.25	SIXI	4.51	2.52	1.45	0.87
56.60	SIXII	2.58	1.52	0.91	0.55
47.30	FeX	9.08	4.63	2.64	1.54
46.60	MgVIII	9.26	4.65
40.80	SIVIII	9.42	4.66
38.50	MgIX	9.79	4.67
37.70	SVIII	10.11	4.68
37.60	FeXII	10.22	4.70
35.70	MgX	10.25	4.86
35.20	SiIX	10.68	5.08	2.70	1.56	0.92
33.80	MgX	11.14	5.20	2.71
33.40	FeXV	11.33	5.29	2.73	1.57
31.60	CV	11.53	5.34	2.77	1.58
30.60	FeXVI	23.73	5.77	2.79
27.55	FeXVII	2.86	1.62	0.93
25.35	FeXVI	2.92	1.66
24.90	SIXII	55.55	17.83	5.38	2.35	1.21	0.67
22.50	NVI	18.12	5.70	2.46	1.25	0.68
18.60	NVII	60.24	19.11	5.75
17.60	SXIV	60.87	21.93	6.84	2.72	1.33	0.71	0.32	0.20	0.13	0.05
16.80	OVII	21.94	7.10	2.91	1.39	0.74	0.33
14.20	OVIII	79.90	36.96	9.92	3.06	1.40
10.40	NeIX	80.00	40.62	19.02	6.46	2.36	1.09
9.16	FeXVIII	41.99	20.49	7.06	2.42
9.12	NeX	7.08	2.50	1.12
8.55	FeXIX	20.63	8.00	3.06	1.80	0.40
7.85	FeXX	3.10	1.36
7.36	FeXXI	3.12	1.45	0.41
7.04	MgXI	1.55	0.45
6.92	FeXXII	21.45	8.89	3.58	1.61	0.46
6.36	FeXXIII	1.65	0.52	0.21
6.33	MgXII	1.66	0.57	0.23
6.06	FeXXIV	8.89	4.02	2.07	0.73	0.29
5.09	SIXIII	2.08	0.97	0.47	0.22	0.06
4.65	SIXIV	22.10	8.99	5.04	2.63	1.07	0.48
3.85	SXV	5.14	3.15	1.58	0.71	0.32
3.56	SXVI	9.22	5.37	3.32	1.67	0.74
2.42	CaXIX	3.35	1.78	0.88	0.40	0.08
1.35	FeXXVI	1.10	0.69	0.19
1.24	NeXXVII	0.21
1.01	NeXXVIII	1.13	0.74	0.24

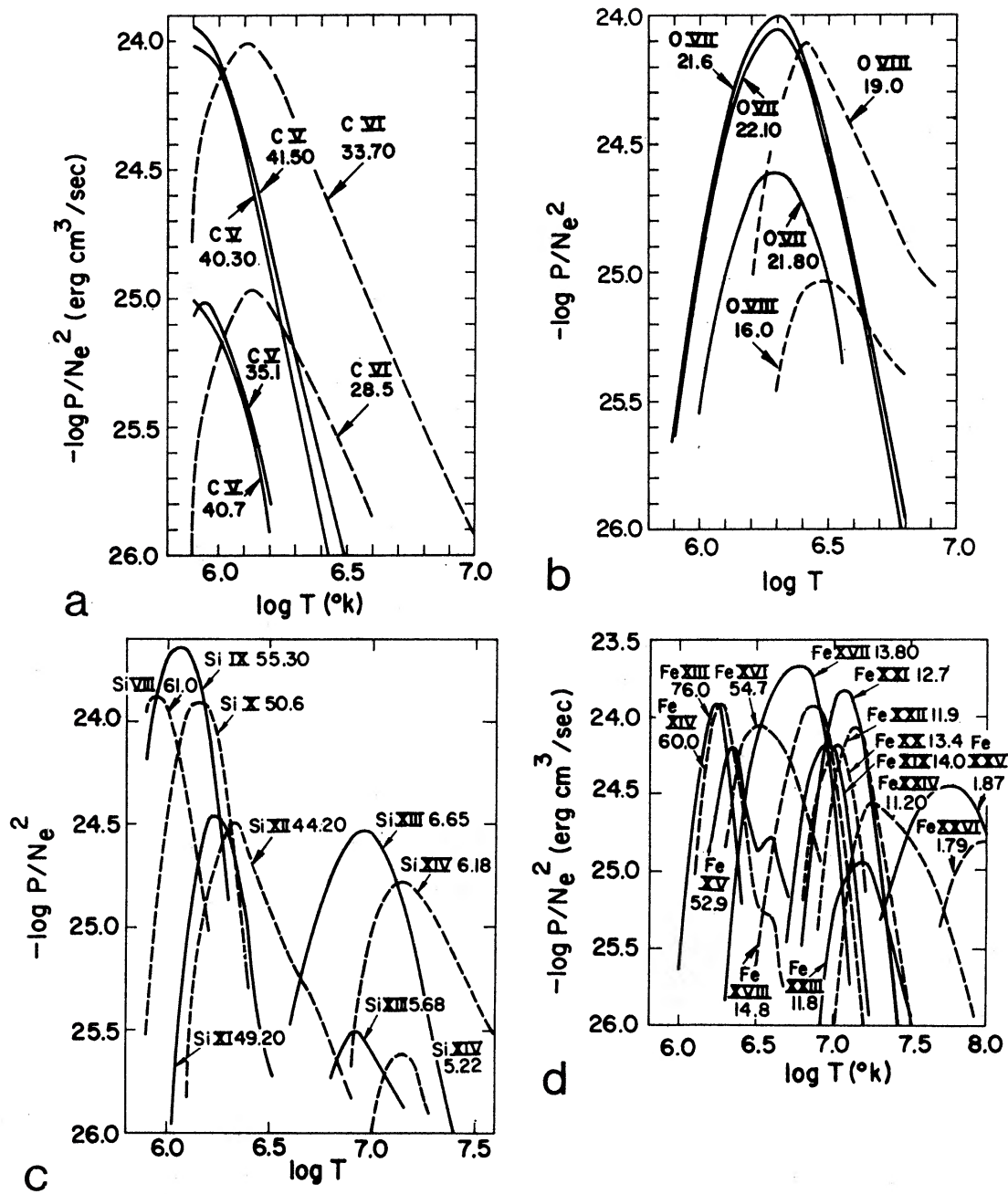


FIG. 3.—Intensity as a function of temperature of some of the strong emission lines. (a) Carbon; (b) oxygen; (c) silicon; (d) iron.

We thank A. Krieger, L. VanSpeybroeck, G. Vaiana, and D. Webb for helpful discussions, H. Chasan for programming assistance, and E. O'Neill for typing a difficult manuscript. This research was supported by NASA contract NASW-2070 and by the Air Force Office of Scientific Research contract F44620-71-C-0019.

REFERENCES

- Allen, J., and Dupree, A. 1969, *Ap. J.*, **155**, 27.
 Beigman, I. L., Vainshtein, L. A., and Vinogradov, A. 1970, *Soviet Astr.—AJ*, **13**, 775.
 Bely, O. 1966a, *Proc. Phys. Soc.*, **88**, 587.
 ———. 1966b, *Ann. d'ap.*, **29**, 131.
 ———. 1967, *ibid.*, **30**, 953.
 Bely, O., and Bely, F. 1967, *Solar Phys.*, **2**, 285.
 Bely, O., and Petrini, D. 1970, *Astr. and Ap.*, **6**, 318.
 Burgess, A. 1961, *Mém. Soc. R. Sci. Liège*, **4**, 299.
 ———. 1965, *Ap. J.*, **141**, 1588.
 Chapman, R. 1969, *Ap. J.*, **156**, 87.
 Connerade, J. 1970, *Ap. J. (Letters)*, **162**, L139.
 Cox, D., and Tucker, W. 1969, *Ap. J.*, **157**, 1157.
 Culhane, J. 1969, *M.N.R.A.S.*, **144**, 375.
 Drake, G., Victor, G., and Dalgarno, A. 1969, *Phys. Rev.*, **180**, 25.
 Elwert, G. Z. 1954, *Zs. f. Naturforschung*, **53**, 637.
 Evans, K., and Pounds, K. 1968, *Ap. J.*, **152**, 319.
 Gabriel, A., and Jordan, C. 1969, *Nature*, **221**, 947.
 Griem, H. 1970, *Ap. J. (Letters)*, **161**, L155.
 Jordan, C. 1966a, *M.N.R.A.S.*, **132**, 463.
 ———. 1966b, *ibid.*, p. 515.
 ———. 1969, *ibid.*, **142**, 499.
 ———. 1970, *ibid.*, **149**, 1.
 Karzas, W., and Latter, R. 1961, *Ap. J. Suppl.*, **6**, 167.
 Kelly, R. 1968, *Atomic Emission Lines Below 2000 Angstroms: Hydrogen through Argon* (NRL Report 6648; Washington: U.S. Government Printing Office).
 Krinberg, I. 1970, *Soviet Astr.—AJ*, **13**, 780.
 Landini, M., and Fossi, B. 1970, *Astr. and Ap.*, **6**, 468.
 Moore, C. E. 1949, *N.B.S. Circ.*, No. 467, Vol. 1.
 ———. 1952, *ibid.*, Vol. 2.
 Pottasch, S. 1967, *B.A.N.*, **19**, 113.
 Rugge, H., and Walker, A. B. C., Jr. 1970, *Space Res.*, **8**, 439.
 Seaton, M. 1955, *Proc. Roy. Soc. London, A*, **68**, 457.
 Shapiro, J., and Breit, G. 1959, *Phys. Rev.*, **113**, 179.
 Shore, B. 1969, *Ap. J.*, **158**, 1205.
 Spitzer, L., and Greenstein, J. 1951, *Ap. J.*, **114**, 407.
 Tucker, W. H., and Gould, R. J. 1966, *Ap. J.*, **144**, 244.
 Walker, A., and Rugge, H. 1970 (preprint).
 Widing, K., and Sandlin, G. 1968, *Ap. J.*, **152**, 545

